

Nearshore Regions of Lake Superior: Multi-element Signatures of Mining Discharges and a Test of Pb-210 Deposition under Conditions of Variable Sediment Mass Flux

W. Charles Kerfoot^{*,1} and John A. Robbins²

¹Lake Superior Ecosystem Research Center and Department of Biological Sciences
Michigan Technological University
Houghton, Michigan 49931

²NOAA Great Lakes Environmental Research Laboratory
2205 Commonwealth Blvd.
Ann Arbor, Michigan 48105

ABSTRACT. Around the turn-of-the century, mining activities greatly increased sediment accumulation and metal fluxes in nearshore regions of Lake Superior. In the low-energy environment of Portage Lake, within the Keweenaw Waterway estuary, sediment accumulation increased 33X, whereas elemental Cu flux increased 312X. One difficulty in establishing the dispersion of mining discharges is that stamp sands were derived from local ore deposits, hence few elements are “unique” to the source materials. One approach is to search for multi-elemental “signatures” in concentration and flux profiles. For example, several rare earth elements of the lanthanide series are characteristic of source materials and have the potential to identify stamp sand material across Lake Superior. Although conditions of variable mass loading from multiple sources can produce complicating dilution effects in concentration profiles, multivariate techniques are capable of deciphering original source signals. Here non-destructive neutron activation analysis was utilized to construct elemental flux and concentration profiles, then multivariate techniques (Factor Analysis, End-member Analysis) were used to illustrate how partial mass flux signatures can be assigned to two different types of ore lodes (conglomerate, amygdaloid) and to background (erosional) sedimentation. Temporal patterns were verified through archived company discharge records. Also exploited were the varve-like deposition of slime clays to independently check ²¹⁰Pb determinations under conditions of variable sediment mass flux and to demonstrate constant excess ²¹⁰Pb delivery to sediments in the presence of massive slime clay loading. The results suggest assumptions of ²¹⁰Pb dating may apply under conditions where sediment accumulation is highly variable.

INDEX WORDS: Metals, Cu, Lake Superior, ²¹⁰Pb, ¹³⁷Cs, Principle Component Analysis.

INTRODUCTION

Of all the Laurentian Great Lakes, Lake Superior contains the strongest development of a separate coastal regime, chemically and biologically distinct from cooler offshore waters. Erosion of metal-rich ore bodies around Lake Superior, either through high-energy shoreline scour or through stream discharge, results in sediments naturally enriched in Cu, Zn, and other elements relative to concentrations characteristic of the lower Great Lakes (Mudroch *et al.* 1988). In addition, turn-of-the-century anthropogenic inputs, largely along the shore-

line, greatly accelerated metal transport and cycling in the basin (Nussman 1965, Kemp *et al.* 1978, Kerfoot *et al.* 1994). Earlier work on sediment cores from the Keweenaw Waterway region of Lake Superior revealed extensive varve-like slime clay layers associated with mining discharges. Realizing the potential for a high-resolution long-term record of mining impacts, a combination of laminae counts and radioisotope dating techniques was employed to contrast Cu concentration and flux profiles in Portage Lake (Kerfoot *et al.* 1994). Evidence was presented that copper-rich sediments extend eastward from the peninsula, along the track of the Keweenaw Current, suggesting the strong current

*Corresponding author. E-mail: wkerfoot@mtu.edu

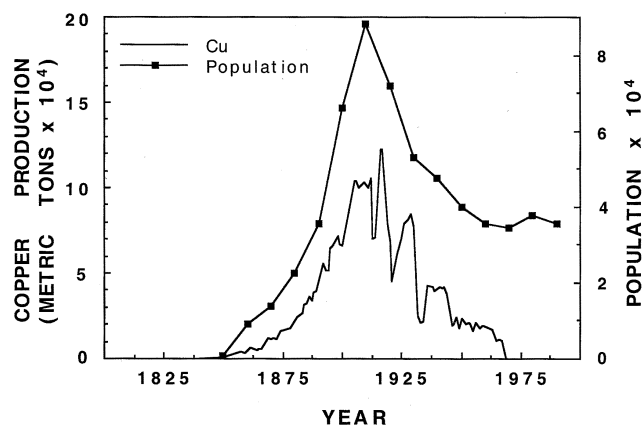


FIG. 1. Relationship between copper production from native copper mining and population size in Keweenaw and Houghton Counties, Michigan (population estimates compiled from Houghton and Keweenaw County records; copper production from Wilband 1978).

dispersed fine particles or dissolved fractions. Chemical characterization of “slime clays” could provide a means of tracing the dispersal of fine particles and the importance of long-shore currents.

One of the first great North American metal mining rushes, native copper mining on the Keweenaw Peninsula (Fig. 1), began in the late 1840s, reached maximum production between 1890 to 1930, and ended in 1968. During that span, 4.8 billion kg (4.8 million metric tons) of copper were produced, with peak output at over 122 million kg (122 thousand metric tons) per year. Between 1850 and 1929, the Keweenaw district was the second largest producer of copper in the world. Although mines stretched for 106 km along the Portage Volcanic Series, over 95% of the total native copper production in the district came from deposits that extended 23 km north and 15 km south of Portage Lake in Houghton County (Babcock and Spiroff 1970).

As the initial copper lodes played out, industry shifted to extracting native copper from poorer ore deposits by crushing the parent rock with mechanical gravity stamps, followed by water-borne gravity separation techniques (Benedict 1955). Use of steam-driven stamp mills allowed the processing of vast volumes of lower grade ore, principally from amygdaloid basalt and conglomerate lodes (Benedict 1952). The concentration of copper in the parent rock processed at stamp mills ranged between 0.5 and 6.1% of total mass, producing vast amounts of discarded stamp sands as a byproduct. Whereas

the crushed rock closely resembled the chemical composition of naturally outcropping bedrock formations, it also contained locally heavy concentrations of metals, particularly copper, and associated characteristic minerals.

Stamp sands were sluiced as water-laden slurries onto stamp sand piles along lake shorelines and into coastal waters. The coarse sand fraction ended up as long-shore bars or beach deposits, subject to further reworking by waves and currents. Clay-sized particles created during the milling process, the so-called “slime” fraction (Lankton and Hyde 1982), dispersed much farther than the sands. The amount of stamp sands delivered to lake sediments largely depended on 1) the proximity and production of mills, and 2) the energy of the depositional environment. In low-energy environments such as the Keweenaw Waterway (Fig. 2), surficial copper concentrations are highest near mill sites, and slime clays from these discharges created artificially laminated lake sediments that preserved a detailed record of heavy metal discharges (Kerfoot *et al.* 1994).

Of the 0.5 Gt of stamp sands deposited around the Keweenaw Peninsula, over 179 million metric tons were discharged into Torch Lake (area = 11 km²). These discharges produced 12 m of bottom clays, as sands and slime clays filled an estimated 20% of the lake volume. In Portage Lake, the deposits were much thinner (0.5 to 1.0 m), primarily because the volume of stamp sands discharged was much less (34 million tons) and the lake was larger (42 km²). Along the higher energy coastline sites, over 80 million metric tons were discharged into Lake Superior directly (5 large mills at Freda-Redridge, 45.5 million; two large mills at Gay, 22.6 million; lesser amounts from two smaller mills north of Baraga).

One approach for identifying sedimentation of mining-derived “slime” clay particles is to determine the rate of delivery of “slime clay” constituents to sediments, i.e., a flux that equals the product of the mass sedimentation rate and the constituent elemental concentrations. The calculations produce elemental flux profiles that emphasize episodes of closely correlated deposition of suspected constituents. The chief difficulty is that stamp sands were derived from local ore deposits, hence few elements are “unique” to the source materials. Another approach is to search for multi-elemental “signatures” in concentration profiles. Although conditions of variable mass loading from multiple sources can produce complicating dilution

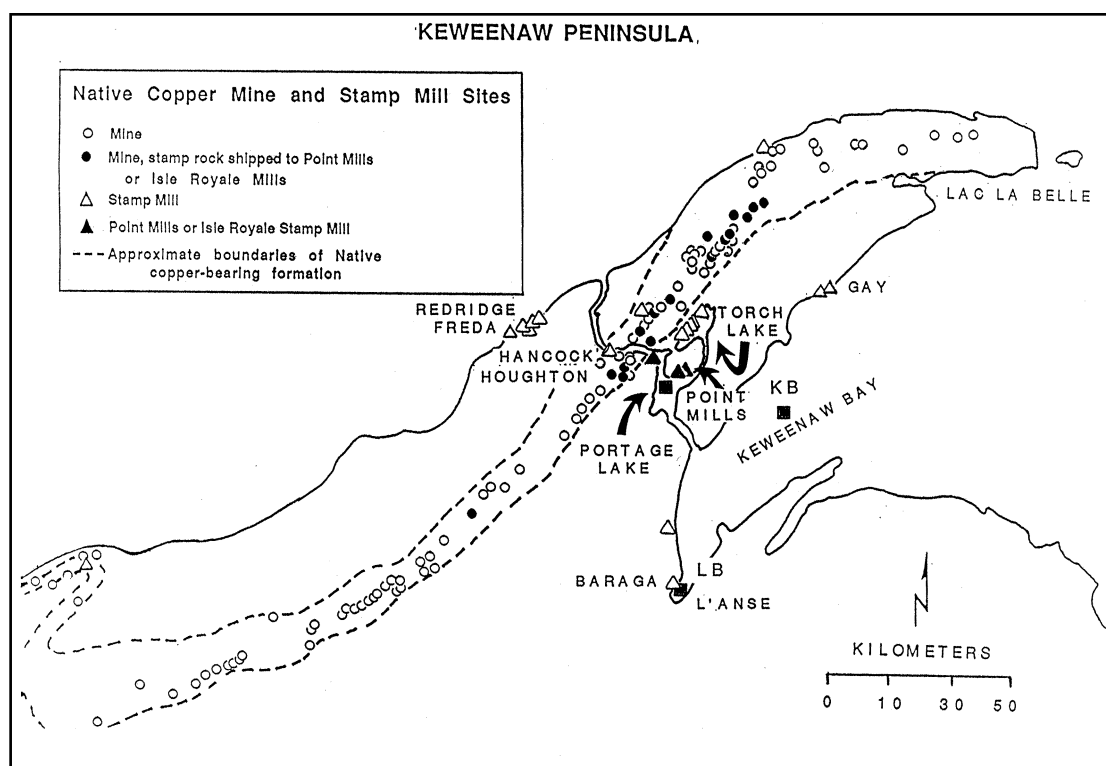


FIG. 2. The distribution of native copper mines along the Portage Volcanic Series and the location of large-volume stamp mill operations along the Keweenaw Waterway and Keweenaw Peninsula. Locations of Torch Lake, Portage Lake, and Point Mills are indicated on the map. Core sites are marked as black squares in Portage Lake (PL #3) and in Keweenaw Bay (L'anse Bay LB; Off Gay, KB); the Whitefish Bay site is offmap 220 km to the east.

effects in concentration profiles, multivariate techniques are capable of deciphering original source signals.

First the varve-like deposition of slime clays was examined to independently check ^{210}Pb determinations under conditions of variable sediment mass flux and to demonstrate constant excess ^{210}Pb delivery to sediments in the presence of massive slime clay loading. Neutron Activation (INAA) techniques, with a few Atomic Absorption Spectrophotometry (AAS) checks, determine individual elemental concentrations. Then distinctive multi-elemental signatures of the slime clays were identified and two separate techniques were utilized for reconstructing sources. Factor Analysis (Principal Components Analysis, with Varimax rotation) was used to characterize multi-elemental flux and concentration profile patterns, clustering elements that coincide with mining discharges from ones that are influenced by other processes, such as diagenesis.

Finally, a multivariate end-member analysis, based on multi-elemental source "signatures" from background sediments and stamp sand samples (conglomerate or amygdaloid ore lodes), was used to reconstruct historical inputs from the two primary ore lodes and erosion. For verification, ore lode loading predictions are compared with documented stamp sand discharge records.

The eventual goal is to characterize the mass and elemental loadings from mining into the coastal zone of Lake Superior and to clarify the time course of processes that influence particle dispersal, dissolution, and eventual deep burial of elemental constituents in basins of net accumulation. Hopefully, the multivariate techniques can be applied to additional core sites across the eastern basin of Lake Superior, to quantify the degree that Cu-rich strata are directly tied to slime clay dispersal from the shoreline sources or are modified by pelagic dissolution and benthic diagenetic processes.

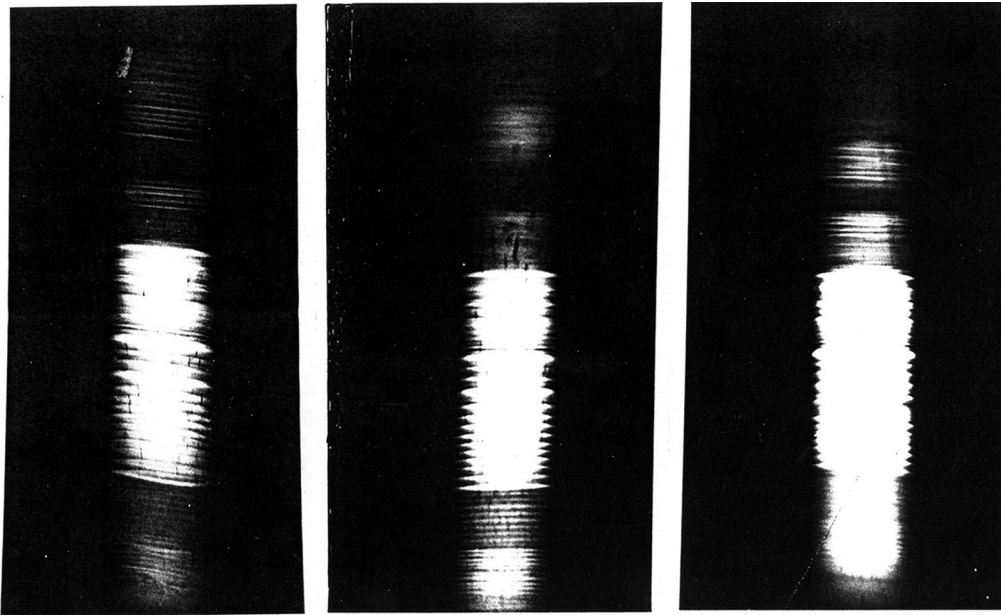


FIG. 3. *Varve-like clay bands in sediment cores from Portage Lake. The Portage Lake cores show three primary regions: a lower purple set of bands derived from about nine early small-volume stamp mills (1855 to 1900), a middle set of 20 thick pink bands derived from three large-volume mills (#2 Franklin, Centennial, Isle Royale; 1900 to 1920), and a final set of thinner light grey bands, interrupted by the Great Depression closings, that trace the final discharges of the Isle Royale Mill.*

METHODS AND MATERIALS

Stratigraphic and Radiometric Determination of Mass Fluxes

In the fall of 1991, several 60 to 70 cm sediment cores were taken in Portage Lake from water depths of 10 to 14 m, using a meter-long 2" Phleger-type KB gravity corer. A Lowrance Model X-16 sonar unit with tape printout helped position the coring device 3 to 4 meters above sediments prior to release. Additional cores were taken during the winter of 1994–5 from Keweenaw Bay, through ice cover, using the same apparatus. Cores were plugged, capped, and transported to Portage View Hospital. At the hospital, they were x-rayed using large and small cassette formats. The large format featured a screened scoliosis cassette (60 kVP peak; 6.4 mAS; DuPont Cronex Quanta III-EG cassette; 14 in. × 36 in. DuPont Cronex 7 film), whereas the small format featured a screened extremity cassette and a non-cassette, unscreened format (extremity cassette: 60 kVP; 20 mAS; DuPont Cronex 7 Quanta Detail-HF cassette; 10 in. × 12 in. DuPont Cronex 7

film; non-cassette: 74 kVP; 1250 mAS; 10 in. × 12 in. Kodak X-Omat TL film). The x-rays disclosed finely varved laminae (Fig. 3).

Sampling and Lead-210 Analysis

Following counting of varve laminae on X-radiographs, cores were sectioned into 1-cm slices, subsampled for microfossil studies and dried at 90°C for radiometric and elemental analysis. Portions of dried, ground sediments were placed in plastic vials of standardized geometry (Robbins and Edgington 1975) and analyzed for gamma-emitting radionuclides (¹³⁷Cs and ⁴⁰K) using a high resolution, planar GE(Li) gamma detector/multichannel analyzer system. Detector efficiency was checked using sediments doped with precisely known (1%) amounts of an NBS-traceable mixed-radionuclide standard solution (Amersham QCY46.1) and counted in the same standard geometry vials. ¹³⁷Cs was determined, from its 661.6 KeV gamma emission, with a precision generally better than 5% for counting times of ~1 d.

One core (PL3 of the original 21-core series) was

selected for detailed ^{210}Pb and heavy metal analyses because 1) the sampling site was closest to the original deep, central basin of Portage Lake, 2) the core had the highest deposition rate and well developed varves, and 3) the ^{137}Cs peak was well-defined (Kerfoot *et al.* 1994) and occurred at the time of its maximum atmospheric fallout based on the analysis of the excess ^{210}Pb profile in post-mining sediments above 12 cm depth. Below this level in the previous paper, varve counting was used exclusively.

The regular varving of sediments in Portage Lake permitted the conventional assumption of the constancy of the excess ^{210}Pb flux to be tested directly (Robbins and Harche 1993). In this heavily impacted system, there are numerous processes which could affect the rate of delivery of excess ^{210}Pb to sediments, including variable contributions from watersheds altered by mining activities, enhanced scavenging of the radionuclide by particles in water flowing through the Keweenaw Waterway into the lake and from mine tailings themselves.

Use of the radiopb dating method depends on the presence of a significant signal of excess ^{210}Pb above background, where the latter results from *in situ* decay of parent ^{226}Ra . Usually background ^{210}Pb is low and can be assumed constant. However, under conditions of low signal to noise ratios, highly variable accumulation rates and possible variations in background ^{210}Pb from mine tailing sources, both ^{210}Pb and ^{226}Ra must be measured. For each sample, 4.00 ± 0.01 g of dry sediment were packed into small counting vials of cylindrical cross section to a constant height (4.00 ± 0.05 cm). Fixing both the geometry and mean bulk density of sediments removed the major sources of variability in efficiency of gamma counting, as small compositional differences have negligible effect. Samples were sealed with radium-free epoxy cement and gamma-emitting progeny allowed to equilibrate with radium for at least 20 days (five half-lives of ^{222}Rn) prior to counting using an intrinsic well detector/multichannel analyzer system. Three photopeaks associated with ^{214}Pb and ^{214}Bi were used (295, 352 and 609 KeV) to determine a single, weighted least-squares average value of ^{226}Ra . ^{210}Pb activity was assessed simultaneously using the 46.5 KeV photopeak. The efficiency of detection was checked using samples of the same sediment spiked with a well-determined amount of NIST standard solution of ^{226}Ra . Uncertainties in determination of ^{226}Ra were 5% or less. The efficiency for detection of ^{210}Pb was checked from the

same ^{226}Ra spike which had a known amount of ^{210}Pb activity arising from in-growth. The amount of ^{210}Pb in the standard solution was determined from an NIST-calibrated ^{210}Pb solution provided by the US EPA. The limit of detection of ^{210}Pb activity is about 0.9 dpm/g. Near the top of the core, uncertainties were about 3% but increased to about 20% in the region of background below about 20 cm depth. It should be noted that the gamma counting method yielded total activities of both isotopes.

When isotopic and mass post-depositional redistribution can be neglected, the activity of total ^{210}Pb at the present time is given by

$$A_T = [F_T(t) e^{-\lambda t} + F_R(t) (1 - e^{-\lambda t})] / R(t) \quad (1)$$

where F_T is the total flux of ^{210}Pb (in dpm/cm²/yr) to sediments at time t in the past, F_R is the flux of ^{226}Ra , R is the total mass flux (g/cm²/yr) and $\lambda = 0.6932/22.26$ yr. The exponential terms account for decay of initial ^{210}Pb and its in-growth from radium. While Eq. 1 is rigorously correct, little meaning can be extracted from the data without introducing the testable approximation that 1) some of the ^{210}Pb arrived in fixed association with ^{226}Ra and 2) that the remainder (excess ^{210}Pb) was delivered at a constant rate. Thus,

$$F_T(t) = F_o + \beta F_R(t). \quad (2)$$

A value of $\beta = 1$ means that the variable part of the total ^{210}Pb flux was in secular equilibrium with ^{226}Ra at the time of deposition. Substituting Eq. 2 into Eq. 1 yields

$$A_T = [F_o e^{-\lambda t} + F_R(t) (1 - (\beta - 1)e^{-\lambda t})] / R(t). \quad (3)$$

Finally defining "excess" ^{210}Pb as $A_T - A_R = A_T - [F_R(t) / R(t)]$, yields

$$A_E = [F_o/R(t) - A_R(\beta - 1)] e^{-\lambda t}. \quad (4)$$

Because the mass flux is independently measured, t can be calculated leaving only two undetermined variables in Eq. 4, F_o and β . A least squares fit to Equation 4 was used to estimate values for F_o and β .

Neutron Activation Techniques

Total concentrations of about 28 elements in dried sediment samples were determined by Instrumental Neutron Activation Analysis (INAA; Dams and Robbins 1970). Small amounts of sample were

irradiated with neutrons using the Ford Nuclear Reactor, University of Michigan, Ann Arbor, at fluxes up to 10^{13} neutrons/cm²/sec for as much as 20 hours. Standards for calibration, co-irradiated with samples, included U.S. Geological Survey rock (Andesite, AGV-1 and Granite, G-2) and National Institute of Standards and Technology (NIST) fly ash (SRM 1633A). The USGS Rock Standards were used to derive instrument measurement errors for 27 elements, both to measure precision and to estimate accuracy. These determinations augmented normal Phoenix Laboratory standards. An extensive table of calibrations is available from the authors on request.

Precision in the determination of elements was less than 5% for many elements (Al, Co, Eu, Fe, Hf, Mn, Na, Sc, Th, Va) and between 5 and 10% for some (Ca, La, Sm, Tb, Ti, Zn). A few were determined with a precision of 10 to 15% (Ba, Lu, Nd, Rb, Ta, Zn) or 15 to 20% (Dy and K). Copper was detected in mining-influenced sediments with a precision of 20% or greater, but not detected in pre-mining samples. INAA generally is not the method of choice for analyzing ppm concentrations of Cu as low concentrations are difficult to determine without high errors. However, the enriched values of Cu in Portage Lake sediments permitted detection, except in pre-mining strata. For this reason, AAS-determined values were used in Portage Lake pre-mining strata and in Keweenaw Bay cores, adjusted by a INAA/AAS least squares regression from the overlapped portion in the Portage Lake core ($Y = 156.6 + 0.557X$, $R^2 = 0.686$). In the Portage Lake core, INAA values were used directly for all other calculations that involve post-1845 strata.

Accuracy in analyses were checked by comparing these analytical results with accepted USGS Rock Standards. Inaccuracies were generally under 5% with the exception of Dy (23% low), Lu (23% low) and Zn (10% high). However these latter biases were within experimental errors in each case.

Factor Analysis

Factor Analysis (Principle Component Analysis; PCA) was used to 1) summarize redundant patterns in elemental profiles for both flux and concentration, and to 2) cluster similar patterns. The PCA technique involves a rigid cosine rotation for multivariate data and can operate on either the correlation or covariance matrix (Sokal and Rohlf 1982). SYSTAT version 5.0 (Wilkinson 1989) was used on

the correlation matrix for 28 elements (both flux and concentration profiles) over 56 cm slices in core PL3 (year interval 1845–1991). It was reasoned that if the stamp rock material remained similar in general composition, then the delivery rate of constituent elements to the sediments would show great autocorrelation. The mining perturbation could then be distinguished by inputs from various sources and separated from diagenetic anomalies.

After PCA on the 24×56 correlation matrix, a Varimax Rotation with the four principal components was performed. Scores for each of the four components were graphed over the 56 sediment depths, and the three closest score profiles plotted along with the three end-member mass fluxes in Figure 11.

Multiple Source (End-member) Analysis: Conglomerate and Amygdaloid Lode Elemental Signatures

Although the long-term goals are to distinguish mill sources, it was tested if it is possible to distinguish between conglomerate and amygdaloid ore sources within the core clay layers, since certain mills specialized on conglomerate ores, whereas others processed only amygdaloid ores. The first step was to sample existing coastal stamp sand piles for INAA analysis. Samples were taken from the original discharge cones by digging 0.5 to 1 m into exposed faces along beachfront margins. The samples considered here include the Mohawk and Wolverine Mill pile off Gay along the shoreline of Keweenaw Bay (which operated from 1902 to 1923, served the Mohawk and Wolverine mines, and mined Kearsarge amygdaloid ore; 2 samples), the Isle Royale pile (1901 to 1947, Isle Royale mill, Isle Royale amygdaloid; 2 samples) and the Franklin #2 mill at Point Mills, both along the shoreline of Portage Lake (1899 to 1918, primarily Franklin Junior Mine, Boston Location, piles of processed Allouez conglomerate and Pewabic amygdaloid; 3 samples; Kerfoot *et al.* 1994 reported stamp pile locations).

The pile samples were used both to indicate the elemental composition of discharges from stamp mill sites and to indicate elemental enrichments in the small particle fraction (slime fraction) most likely to be carried the furthest across the lake and deposited onto bottom sediments. Wet sediments were sieved through 177 μ m mesh Nitex. Portions (ca. 2 g) of the < 177 μ m fraction were resuspended

with 250 mL of distilled water in 30-cm-tall graduated cylinders. Particles were allowed to settle for 4 days, sufficient time to allow most particles with mean diameters of 1 mm or greater, and with assumed densities of 2.6 g/cm³, to settle out according to Stoke's Law. Each supernatant was then centrifuged for 1 hr at ca. 10³ G. The residue was collected from a sufficient number of tubes (4) to prepare replicate samples (100 mg dry wt. each) for INAA analysis. The results from the < 1 μm size fraction were compared to the < 177 μm size fraction by calculating a simple enrichment ratio (concentration < 1 μm / concentration < 177 μm). Copper and zinc were highly enriched in the slime fraction, followed to lesser degrees by cobalt, arsenic, and manganese. Chromium was slightly enriched, whereas silver was highly enriched in the Point Mills sample, but not in others.

Three principal sources of sediment to the coring site were considered: natural pre-mining material (background lake sediment) and fines from Point Mills and Isle Royale stamp sands. The pile samples came from the two primary rock types, which were also distinguished by color: conglomerate (purple) and amygdaloid (dark grey) lodes. Each source is assumed to contribute a time-varying flux to sediments designated by $F_s(t,k)$ (with $k = 1, 2, 3$) where t is the time before present and k indexes the sources. If $C_s(k,m)$ is the concentration of the m th element in the fine fraction at the k th source, then the total flux of element m to the coring site is

$$F_s(t,1)C_s(1,m) + F_s(t,2)C_s(2,m) + F_s(t,3)C_s(3,m). \quad (5)$$

Note it is assumed that $C_s(k,m)$ is not time-dependent. If there are no other sources then this sum must be equal to the product of the mass flux, $F(l)$, to the site and the measured concentration of the element $C(l,m)$ in the l th depth interval which is,

$$F(l)C(l,m) = \sum_{k=1}^3 F_s(l,k)C_s(k,m). \quad (6)$$

In Eq. 6 the "t" in term $F_s(t,k)$ was replaced with $F_s(l,k)$, because every level (sediment core section) corresponds to a time t when the flux from the source is given by $F_s(t,k)$. Since $F(l)$ is measured in the present study as well as $C(l,m)$, values of $F_s(l,k)$ were sought which minimize the weighted square of the difference between the left hand and right hand sides of Eq. 6 summed over all elements. That is, values of $F_s(l,k)$ are found which minimize for each level l ,

$$V(l) = \sum_{m=1}^{24} \left[\frac{F(l)C(l,m) - \sum_{k=1}^3 F_s(l,k)C_s(k,m)}{\sigma(m)} \right]^2 \quad (7)$$

where $\sigma(m)$ is the characteristic uncertainty in the determination of values of $C(l,m)$ derived from counting errors. This multiple source analysis method is thus a modified chi-squared minimization with an analytic solution. Uncertainties in estimated source fluxes were calculated by Monte Carlo methods. To do this, 100 sets of trial values of the sets of $C(l,m)$ and $C_s(k,m)$ were generated with $m = 1, 24$, assuming that such values were normally distributed around each original value with a standard deviation given by the counting errors. A mean value was then calculated for 100 sets of the three optimized source loadings, $F_s(k,1)$, $k = 1,3$, and the associated standard deviation was reported as the uncertainty for each value.

Determination of Historical Stamp Sand Discharges

The Copper Country Archives section of the J. R. Van Pelt Library, Michigan Technological University, retained copies of historical processing records for many copper mining companies. The archived records include yearly and occasionally monthly reports of total Cu produced, total amount of rock mined from various lodes, and total amount of rock shipped to stamp mill operations. These records allowed reconstruction of the total amount of stamp rock processed and determination of the fraction from conglomerate and amygdaloid lodes. Yearly total stamp sand production for several mills is given in Kerfoot *et al.* (1994).

RESULTS

Lead-210 Analysis

The total activity of ²¹⁰Pb (Fig. 4a) declines from a maximum of about 30 dpm/g at the surface to levels supported through decay of radium (0.5 to 4.0 dpm/g) at about 20 cm depth. Below 20 cm, ²¹⁰Pb and ²²⁶Ra are essentially in secular equilibrium as evidenced by the equality of specific activities. As expected, the activity of ²²⁶Ra is not constant over the length of the core but varies in response to impacts of mining activities and the multiplicity of source materials. Over most of the core length, radium tracks extremely well with potassium (Fig. 4b), as measured by its long-lived radioactive iso-

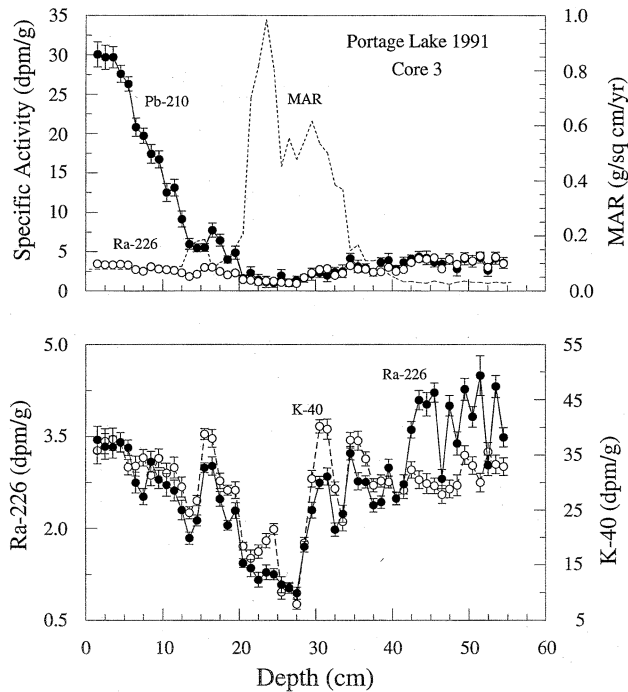


FIG. 4. Depth relationships of radionuclide activity in PL #3: a) specific activity of ^{210}Pb (solid dots) and ^{226}Ra (open circles) plotted with mass accumulation rate (MAR), b) ^{226}Ra (solid dots) and ^{40}K (open circles) activity, showing dilution effects between 12 to 16 and 18 to 40 cm depth.

tope, ^{40}K ($t_{1/2} = 10^9$ years). Radium diverges from potassium in the lower 15 cm of the core, in pre-mining (background) sediments. Since the activities of ^{226}Ra and ^{40}K vary inversely with total mass flux (compare Figs. 4a and 4b), it is evident that tailing slimes are depleted in radium and potassium relative to background materials and that the slime clays dilute the activity of these isotopes.

A least squares fit of Eq. 4 to the measured values of A_E yields $F_0 = 2.62 \pm 0.05$ dpm/cm²/yr and $\beta = 1.0 \pm 0.04$. The analysis shows that the variable part of the ^{210}Pb flux is in secular equilibrium with radium ($\beta = 1.0$). The resulting excess ^{210}Pb profile is in excellent accord with observation (Fig. 5a). Through the region of variable sedimentation below 3.0 g/cm² (ca. 20 cm) the model calculation tracks well with observations.

Given that $\beta = 1$, values of F_0 may be calculated from Eq. 4 as

$$F_0 = A_E R(t) e^{+\lambda t} \quad (8)$$

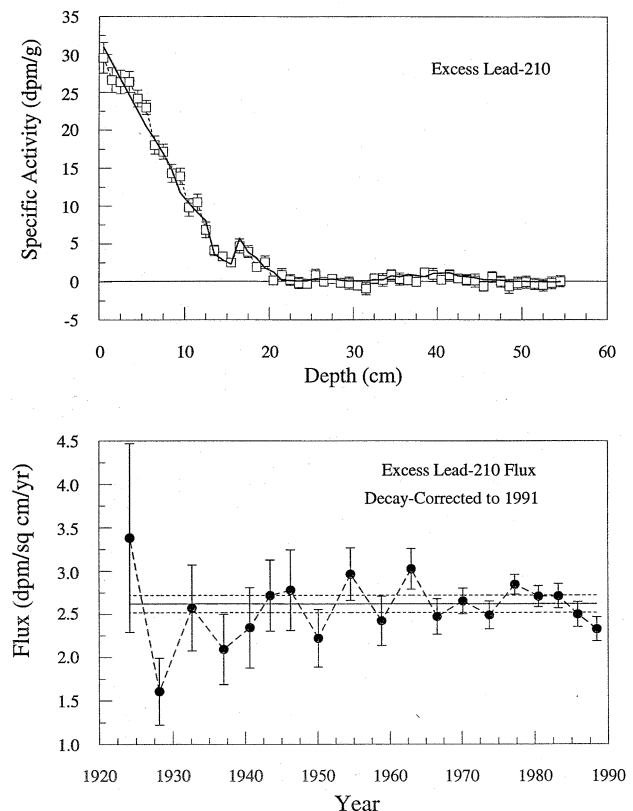


FIG. 5. Excess ^{210}Pb activity: a) expected (—) versus observed (\square) specific activity of excess ^{210}Pb plotted against depth, and b) excess ^{210}Pb flux plotted against date for the interval 1920 to 1990, showing time-independence within experimental error.

The result is that between 1920 and 1990, the flux of excess ^{210}Pb to the coring site was time-independent within experimental error, despite a several-fold change in mass flux during the period (Fig. 5b).

Mass Sedimentation

Sediment mass flux (g/cm²/yr) was estimated down to a depth of 55 cm. Values down to 1850 are shown in Figure 4a. The presettlement (background) mass flux at the center of the lake was relatively low, averaging around 0.03 g/cm²/yr. Sedimentation more than tripled to 0.11 g/cm²/yr during the early copper mining years (1850 to 1890). Background sediment load increased from deforestation associated with early mining activities (see end-member analysis), as period photographs document barren hillsides around the waterway

(Lankton and Hyde 1982, Lankton 1991). However, purple clay banding suggests that a substantial bulk of the increased mass flux came from early stamp mill operations, especially contributions from milling the conglomerate lode (contributions of Franklin #1 Mill). In the early days, mills were located near the cities of Houghton and Hancock, more distant from the center of the lake than later operations, and processed much less material than later mills (Kerfoot *et al.* 1994).

With the opening of large-volume stamping mills that discharged directly into the northern and central basin of the lake, there was another several-fold increase in sediment accumulation, principally coming from discharged mill slime clays. Three large mills discharged directly into Portage Lake, mixing slime clays from amygdaloid and conglomerate sources to produce a characteristic set of twenty pink bands. The two large-volume Point Mills (one processing amygdaloid lode stamp rock, the other a mixture of amygdaloid and conglomerate lode rock) and the Isle Royale (amygdaloid only) stamp mills operated simultaneously (Kerfoot *et al.* 1994). Mass flux peaked between 1909 and 1917 at $0.99 \text{ g/cm}^2/\text{yr}$. Sedimentation decreased dramatically after the Point Mills operations closed in 1919 and after the last mill, the Isle Royale Mill, reduced operations in 1920 and finished discharging in 1947. At present, mass flux has declined to $0.05 \text{ g/cm}^2/\text{yr}$, slightly above pre-mining values (0.02 to $0.04 \text{ g/cm}^2/\text{yr}$, Table 1).

Elemental Flux and Concentration Profiles

The precise dating allowed assignment of time horizons to depth strata, and the calculation of detailed flux and concentration profiles for individual elements (Table 1). The variable mass flux conditions and the temporal variations in source materials make the flux and concentration profiles of trace elements differ from one another (Figs. 6 and 7).

High 1900 to 1920 loading is indicated for calcium and sodium, two major mineral constituents of basalt, rare earth and related elements (europium, hafnium, and tantalum), and barium (Fig. 6). In the right panel, copper also follows the basic historic loading pattern, but cesium and arsenic are conspicuously different. The latter two elements have later, broader peaks. Note that the concentration of cesium refers to the stable element and is essentially unrelated to ^{137}Cs that originated from nuclear weapons testing.

Concentration profiles are illustrated in Figure 7.

Concentration peaks of calcium and sodium are broader than flux profiles, rare earths show different timing patterns, and copper remains high up to the present. Cesium declines in concentration during the 1900 to 1920s sediment pulse, as does arsenic, suggesting strong to moderate dilution effects.

Most flux profiles showed very high correlations. Many elemental flux profiles are highly correlated with known bulk loading from stamp sand discharges, simply because stamp sand production and total mass flux were highly correlated. Pairwise correlations emphasize the similarities. Within the 1853 to 1989 interval ($N = 55$ values), ten elements show correlations above 0.9 (Co, Sc, Fe, Cr, Na, Mn, Ca, Al, Zn, Lu), ten between 0.8 and 0.9 (Eu, Yb, Ba, Se, Tb, Dy, Hf, Sm, Ce, La), five between 0.7 and 0.8 (Nd, Ta, Cu, Th, Rb), and one between 0.6 and 0.7 (K). Many of the highest correlations are for elements found in basalt, rare earths, or metals enriched in the lode deposits. A few exceptions stand out. Correlations for Cs (0.354) and As (0.326) are noticeably lower.

Enrichment values can be calculated for individual elemental fluxes, using background values from the earliest, basal varves (Fig. 8; Table 2). Of all the elements, copper flux stands out as noticeably elevated, increasing to a maximum 312X above background values during maximum historic stamp sand discharges (1900 to 1919) and remaining 18 to 25X above background in the top five centimeters depth. Other highly enriched fluxes during stamp sand discharge maxima include Ca (175X), Co (139X), and Zn (67X). Summary statistics are listed in Table 2. Division of maximum values by minimum values emphasizes the fluctuations of Cu (37X), with As (18X) and Cs (15X) also high. Coefficients of variation ($CV = SD/\text{mean}$) are high for As (100), Cu (70) and Ca (59). Because copper is so enriched relative to zinc, these results suggest that the ratio of Cu/Zn may provide a valuable index of mining disturbances in sedimentary strata.

Factor Analysis: Patterns for Flux and Concentration Profiles

Factor analysis was used to objectively summarize multi-element flux patterns. Unfortunately, flux profiles were so dominated by the yearly slime clay discharges, which caused a 33-fold variation in mass sediment flux downcore, that multivariate techniques merely underscored the redundancy between flux profiles. PCA analysis of elemental flux profiles showed a strong clustering of 26 of the 28

TABLE 1. Sediment mass flux and elemental composition calculated from core PL3. All elemental concentrations by Neutron Activation Analysis. Slices are at 1-cm depth intervals. INAA values for copper below 43 cm level are not reliable.

Slice	Date At		Sed Flux (g/cm ² /yr)	Elements (µg/g)															
	Mid Slice	At		Al	As	Ba	Ca	Ce	Co	Cr	Cs	Cu	Fe	K	Mn	Na	Zn		
1	1,989.5		0.0468	69,500	19.7	675	13,280	84.8	28.8	102	4.8	1,074.0	64,900	16,200	2,746	8,020	NR		
2	1,986.1		0.0593	71,500	20.5	459	10,630	87.8	29.9	103	4.5	1,212.0	72,000	17,500	2,617	8,130	175.4		
3	1,982.8		0.0625	68,500	23.3	788	10,640	90.1	30.9	105	4.2	740.0	61,800	22,000	2,277	8,310	160.2		
4	1,979.4		0.0604	71,500	23.7	800	11,700	89.3	31.2	105	5.5	675.9	68,800	20,900	2,361	8,030	205.0		
5	1,976.0		0.0675	73,500	25.7	734	12,140	84.8	30.0	105	3.9	1,008.0	67,200	19,700	2,413	8,200	207.6		
6	1,972.7		0.0843	66,300	28.9	646	10,580	91.7	31.9	108	4.6	895.4	70,900	25,700	2,189	8,310	185.3		
7	1,969.3		0.0794	67,800	34.1	665	13,240	94.3	34.1	113	5.2	1,160.0	71,200	21,300	2,093	8,460	195.1		
8	1,966.0		0.0909	69,800	40.9	531	14,400	80.6	33.7	106	3.5	1,201.0	65,300	19,900	2,037	8,670	190.6		
9	1,962.6		0.0786	74,100	52.9	641	15,190	82.7	40.1	119	4.2	1,191.0	72,600	15,200	2,076	9,460	204.1		
10	1,959.2		0.1015	75,400	54.3	446	13,840	76.8	40.2	117	5.0	1,521.0	70,700	19,200	1,959	9,620	203.2		
11	1,955.9		0.1177	74,800	63.3	457	15,260	80.1	42.4	122	3.9	1,238.0	71,300	12,200	1,851	10,200	176.3		
12	1,952.5		0.1091	72,900	84.6	524	14,450	90.8	47.9	127	3.6	1,518.0	73,600	23,700	1,784	10,300	222.0		
13	1,949.2		0.1287	76,700	92.5	599	18,850	79.6	52.7	138	2.7	1,166.0	79,400	18,500	1,907	10,800	239.9		
14	1,946.1		0.1628	82,200	39.5	296	23,740	64.7	66.5	198	2.5	1,943.0	96,500	18,000	1,900	10,100	222.9		
15	1,943.3		0.1812	85,200	24.9	387	25,690	61.4	59.0	177	2.5	1,027.0	88,100	16,000	1,894	9,790	206.7		
16	1,940.5		0.1879	82,100	36.8	649	18,170	86.8	45.2	142	4.8	1,431.0	75,800	23,000	1,628	9,090	207.6		
17	1,936.8		0.0810	75,600	71.4	502	16,830	116.0	44.8	135	4.8	1,379.0	72,800	19,700	1,612	9,290	260.4		
18	1,932.4		0.1034	83,100	63.2	337	22,420	83.2	55.1	176	4.0	1,586.0	79,200	15,000	1,894	9,020	257.8		
19	1,928.0		0.1137	86,700	41.0	281	24,910	71.5	63.0	186	2.6	942.2	87,800	12,400	1,886	9,270	187.1		
20	1,924.0		0.1597	84,700	31.0	244	24,110	67.6	55.7	162	2.3	977.6	82,400	15,900	1,852	8,870	257.8		
21	1,920.5		0.2078	79,400	15.2	283	38,080	70.5	69.4	179	0.8	803.4	103,800	10,700	1,898	11,300	222.9		
22	1,918.3		0.7010	76,700	9.7	308	40,090	72.6	68.2	166	0.4	1,092.0	104,400	6,700	1,874	12,400	165.6		
23	1,917.2		0.8192	74,400	7.4	313	36,460	85.1	71.0	165	0.5	746.5	110,300	8,700	1,704	13,900	244.3		
24	1,916.3		0.9848	77,500	7.6	320	44,710	86.9	64.5	153	0.6	987.0	105,100	5,600	1,745	13,600	182.6		
25	1,915.4		0.8037	78,800	9.0	314	32,450	82.4	73.8	167	1.0	689.1	111,200	12,900	1,673	12,700	214.8		
26	1,914.0		0.4522	72,000	6.2	278	49,130	59.4	64.9	143	0.6	543.3	110,500	5,200	1,783	13,700	180.8		
27	1,912.4		0.5543	71,300	7.0	331	45,710	57.0	75.6	164	0.5	473.3	119,400	7,600	1,781	14,000	228.2		
28	1,910.9		0.4770	68,700	6.1	344	40,930	62.4	73.1	166	0.4	718.6	121,800	8,500	1,680	17,200	181.7		
29	1,909.6		0.8443	67,000	6.3	278	43,460	103.0	60.2	139	0.5	845.2	106,800	11,200	1,586	18,500	231.8		
30	1,908.1		0.6160	68,000	2.0	420	36,360	149.0	58.4	132	1.1	876.8	104,400	21,100	1,446	17,000	245.2		

(Continued)

TABLE I. Continued.

Slice	Date At		Sed Flux (g/cm ² /yr)	Elements (µg/g)													
	Mid Slice	Al		As	Ba	Ca	Ce	Co	Cr	Cs	Cu	Fe	K	Mn	Na	Zn	
31	1,906.5	66,800	0.5340	5.4	468	32,730	178.0	48.6	117	0.5	1,433.0	91,700	28,900	1,300	15,900	213.9	
32	1,904.5	69,900	0.5009	5.2	456	30,130	152.0	47.3	110	1.1	1,121.0	91,600	23,400	1,493	14,900	258.7	
33	1,902.4	73,900	0.3642	5.4	302	33,510	111.0	61.0	136	0.8	1,176.0	104,200	12,300	1,781	13,600	230.0	
34	1,900.3	70,400	0.3682	7.3	270	39,350	111.0	62.2	128	0.8	1,659.0	97,300	16,800	1,893	13,300	267.6	
35	1,897.7	78,600	0.1466	7.4	600	22,540	176.0	66.2	131	2.0	2,868.0	83,500	17,700	1,984	12,400	356.2	
36	1,894.4	73,400	0.1675	5.9	455	22,100	166.0	66.6	129	1.6	2,209.0	86,800	20,100	2,006	10,700	300.7	
37	1,890.6	75,000	0.1094	6.2	446	25,090	149.0	72.7	136	2.0	2,447.0	100,000	21,100	2,161	10,100	337.4	
38	1,885.9	71,000	0.1100	6.5	274	26,200	99.6	73.9	128	1.8	1,484.0	100,200	17,700	2,328	9,830	267.6	
39	1,880.8	68,600	0.1141	16.0	583	24,700	109.0	76.1	128	1.5	1,504.0	108,500	17,300	2,188	9,760	223.8	
40	1,874.3	67,300	0.0608	19.1	460	22,320	96.4	53.1	103	3.1	949.4	89,900	20,000	1,999	8,340	199.6	
41	1,865.4	64,900	0.0465	21.8	701	17,800	91.8	38.6	96	2.4	713.4	75,400	18,500	1,748	7,330	139.6	
42	1,855.4	60,800	0.0329	16.5	657	11,620	106.0	24.1	82	3.1	493.8	65,800	16,900	1,609	6,170	125.3	
43	1,845.4	57,400	0.0345	9.8	693	9,220	96.0	15.9	70	4.3		54,800	17,800	1,535	5,460	111.9	
44	1,835.4	58,700	0.0298	6.6	924	8,110	104.0	14.5	74	4.3		55,700	19,100	1,644	5,370	92.2	
45	1,825.4	56,900	0.0283	6.5	554	8,300	106.0	14.6	75	4.2		56,800	16,400	1,517	5,200	92.2	
46	1,815.4	56,600	0.0357	7.8	767	9,270	102.0	14.1	73	3.9		54,100	13,100	1,542	5,330	94.0	
47	1,805.4	56,800	0.0299	6.4	837	8,150	108.0	15.0	78	3.4		59,800	12,100	1,504	5,010	88.6	
48	1,795.4	56,700	0.0240	6.0	686	6,950	107.0	13.8	71	4.1		55,500	17,000	1,446	5,280	118.1	
49	1,785.4	54,900	0.0316	7.1	703	6,660	107.0	14.3	69	3.8		56,100	12,200	1,511	5,360	92.2	
50	1,775.4	55,800	0.0362	7.5	639	7,760	105.0	14.7	73	4.1		56,900	19,800	1,517	5,300	86.8	
51	1,765.4	58,300	0.0322	8.1	537	7,450	104.0	14.7	75	3.7		57,000	18,900	1,489	5,550	104.7	
52	1,755.4	59,500	0.0322	6.9	746	10,070	102.0	14.3	75	4.3		56,700	21,000	1,457	5,460	90.4	
53	1,745.4	62,900	0.0283	8.2	681	9,190	111.0	15.3	83	4.7		60,600	19,100	1,479	5,810	94.0	
54	1,735.4	58,200	0.0334	6.9	855	6,300	113.0	15.9	76	4.4		65,600	14,800	1,664	5,670	91.3	
55	1,725.4	61,800	0.0295	7.6	575	9,100	107.0	14.9	71	4.4		54,900	22,900	1,459	5,770	120.8	

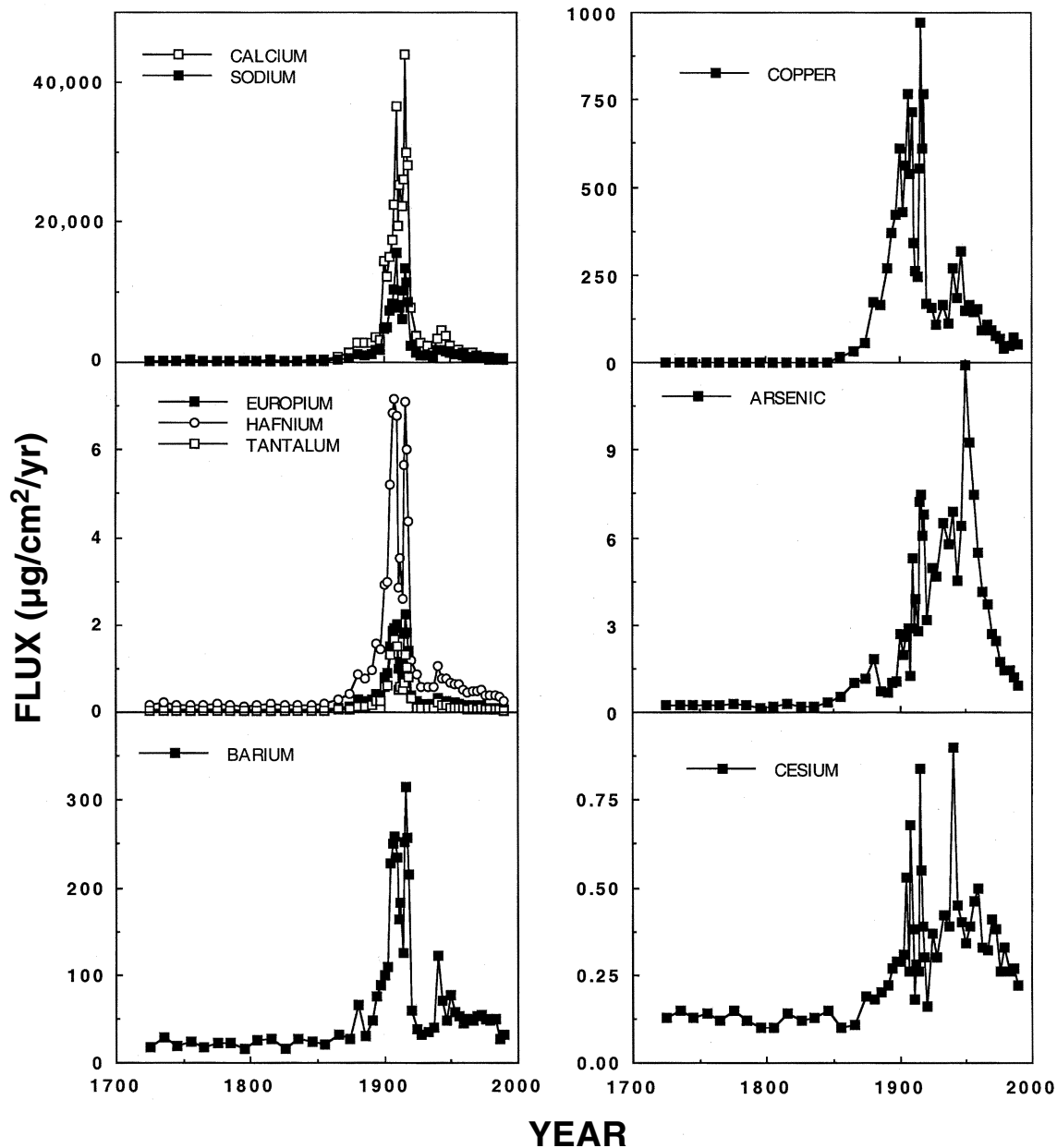


FIG. 6. Selected flux profiles from the Portage Lake core: calcium, sodium, europium, hafnium, tantalum, barium, copper, arsenic, and cesium.

elemental profiles on the first eigenvector (Fig. 9a). The first eigenvector explained 86.3% of the variance, emphasizing the importance of mining impacts to the overall core flux record. Profiles from only three elements (cesium, arsenic, and potassium) loaded strongly on the second (As 0.876, Cs 0.630) and third eigenvectors (Cs 0.652, K 0.407). The second and third eigenvectors explained 5.5 and 4.4%, respectively, of the total variance. Com-

ponents from the first five eigenvectors explained 98.5% of the total flux variance. The simplest interpretation of the PCA flux pattern is that the first vector represents stamp sand discharges, strongly correlated with mass flux. Loading on the second and third eigenvectors separated out profiles with flux maxima later than 1920, and were possibly sensitive to elements influenced by diagenesis (Mn, As).

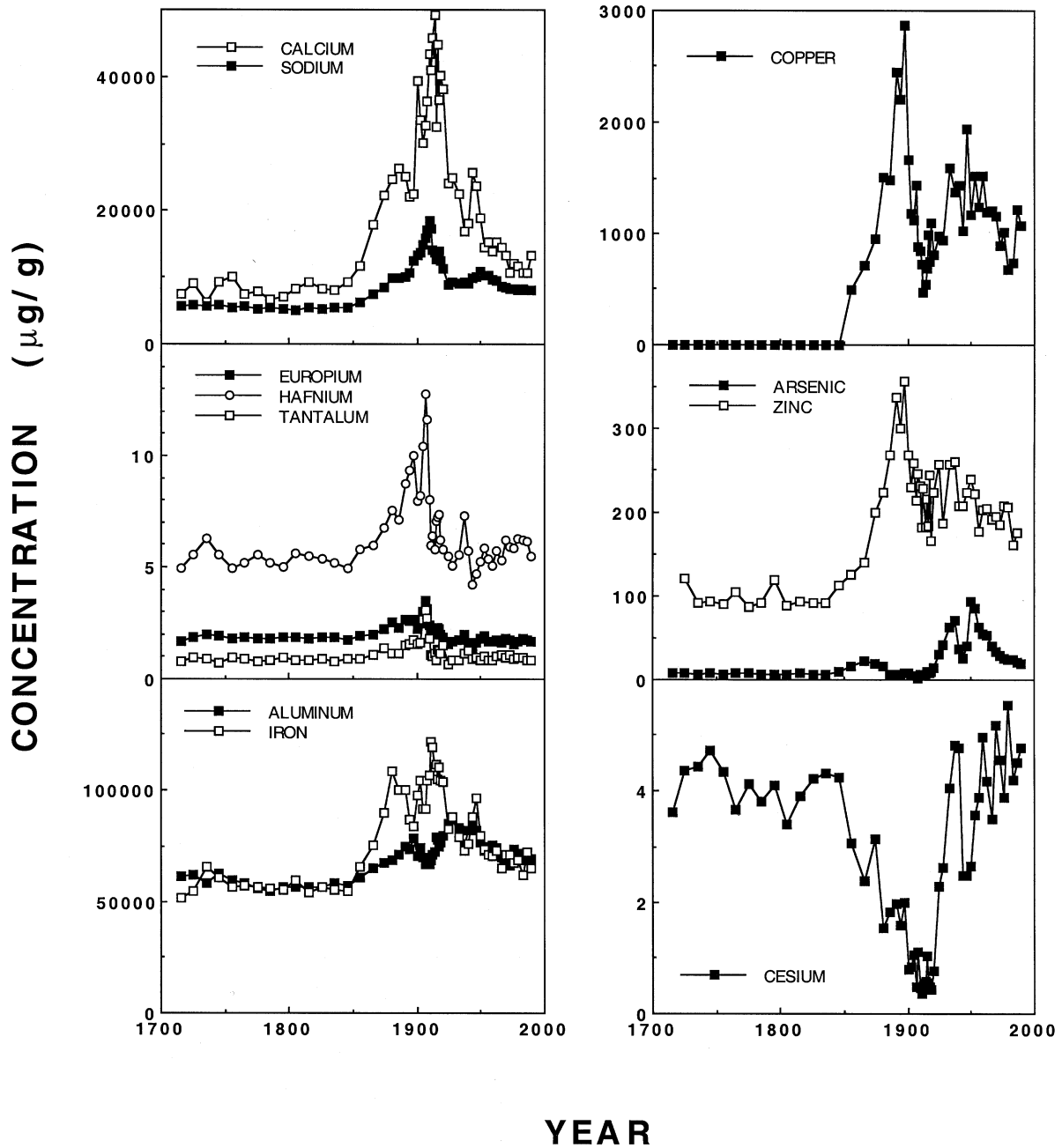


FIG. 7. Selected concentration profiles from the Portage Lake core: calcium, sodium, europium, hafnium, tantalum, aluminum, iron, copper, arsenic, zinc, and cesium.

The PCA for concentration profiles revealed a much wider variety of patterns and a corresponding spread of eigenvectors (Fig. 9b). The eigenvalue for the first eigenvector explained 43.8% of the total variance and the second 28.4%. Component loadings declined after the first four factors, as accumulative component loadings on the first five eigenvectors explained 89.6%.

An assemblage of rare earths and related elements (Factor #1), the “Sm group” profiles (Sm, La, Ce, Tb, Eu, Nd, Hf, Yb, Lu, Ta, Dy, and Th) load positively on the first eigenvector (close to 1.00). Elements of this group show concentration peaks around 1900 followed by return to initial conditions by the 1920s (Sm, Fig. 8). The pattern suggests the influence of conglomerate lodes from

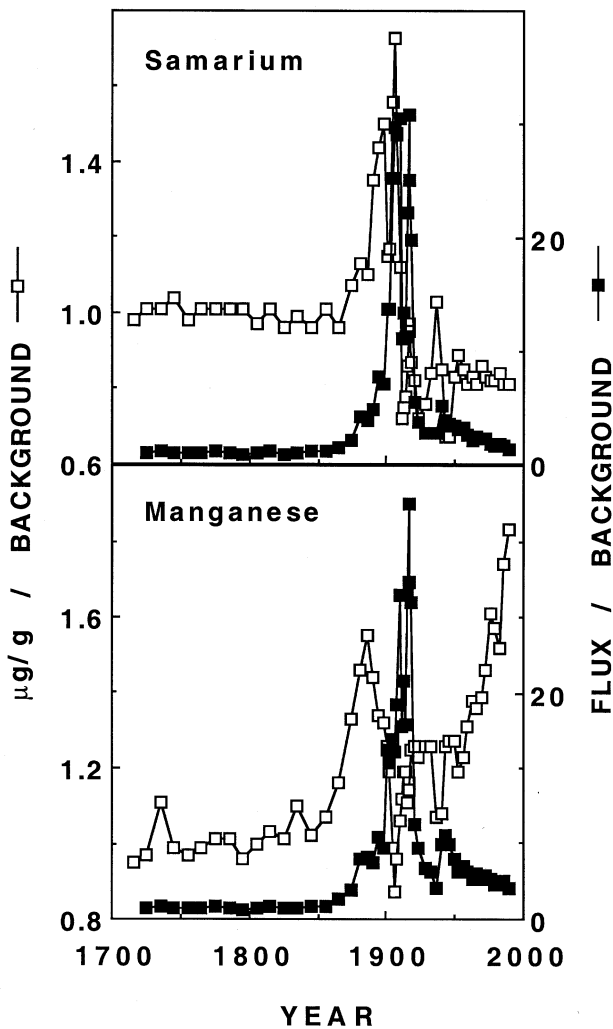


FIG. 8. *Relative flux and concentration profiles for samarium (Sm) and manganese (Mn). Here the values are rescaled by background (premining) values to emphasize enrichment values.*

the Franklin Mill discharges, that contributed greatly to early discharges yet declined during the early part of the century.

The second eigenvector (Factor #2) contains a group that shows behavior similar to (Fe, Cr, Na, Co, Ca, Sc) or opposite from iron (Cs, Ba, Rb), the “Fe group” profiles (Fig. 9b). Whereas Factor #1 shows few dilution effects, Factor #2 contains “diluter” and “diluted” profiles. The first cluster of elements (Fe, Cr, Na, Co, Ca, Sc) is mainly part of Factor #2 (close to 1.00) with very little of Factor #1, whereas Cs and, to a lesser extent, Ba and Rb are also in Factor #2, but negatively loaded (close to -1.00) with very little admixture of Factor #1.

The temporal pattern for the “Fe group” cluster is trimodal, with a primary peak slightly after 1900 surrounded by secondary peaks around the 1880s and 1940s. Factor #2, the Fe group, seems to be identifying elements characteristic of the amygdaloid lode discharges, emphasizing the late 1880–90s shutdown, large mill discharges between 1900 to 1920, and the re-emergence of activity in the exclusively amygdaloid operations of the Isle Royale Mill during WWII.

Finally there are “outliers” (As, Mn, Al, Cr, Cu, Zn, and K). Al (0.779), Cu (0.728), Zn (0.683), Cr (0.540), Co (0.427), and Th (0.364) load positively on Factor #3, whereas only Mn (-0.725) and As (0.456) contribute substantially to Factor #4. Mn shows noticeable enrichment near surface strata (Fig. 8). As and Mn also exhibit dilution effects and load negatively on Factor #2.

One intriguing possibility, mentioned earlier, is that the factor loadings begin to separate out source effects. Factor #1, the Sm group, could be distinguishing suites of elements characteristic of the early mill processing, particularly the conglomerate lodes. Factor #2 may be influenced more heavily by amygdaloid lode discharges. Factor #3 could be distinguishing some components of background sedimentation, whereas Factor #4 might be highlighting diagenetic effects. The PCA results of 24 elements \times 56 depth matrix produced four principle components which were then subjected to a Varimax Rotation (SYSTAT; Wilkinson 1989). Scores for each of the four components were correlated with corresponding partial mass fluxes from the end-member analysis and plotted in Figure 11. However, because of orthogonal constraints on PCA analysis, a better approach to revealing sources was to conduct a formal end-member analysis, directly utilizing stamp rock source materials.

INAA Analysis of Tailing Pile Slime Fractions

The general composition of stamp sands was checked elsewhere by AAS (Kennedy 1970). In general, as expected from the elemental composition of basalts, the elements silica, iron, aluminum, calcium, potassium, sodium, and magnesium are most abundant in stamp sands. Titanium, copper, silver, and manganese are also common components.

Two representative examples of the seven INAA analyses of stamp sand pile samples are shown in Tables 3 and 4, one representing the conglomerate lode and the other the amygdaloid lode material.

TABLE 2. Summary characteristics of elemental concentration and flux profiles at site PL3 in Portage Lake. Concentrations are totals determined by neutron activation reported in units of $\mu\text{g/g}$ unless otherwise indicated whereas fluxes are reported in units of $\mu\text{g/cm}^2/\text{yr}$. Range of enrichment values (concentration, flux) given for top five centimeters.

Element	Concentration					SD/Mean (%)	Concentration Present/Bkgr	Flux:	
	Minimum	Maximum	Max/Min	Mean	Std. Dev.			Peak/Bkgr	Present/Bkgr
Al (%)	5.49	8.67	1.6	7.00	0.85	12	1.2–1.3	42.4	1.8–2.7
As	5.20	93.00	10.0	21.00	22.00	100	2.7–3.6	33.5	4.1–7.7
Ba	244.00	920.00	3.8	530.00	180.00	35	0.7–1.2	14.7	1.5–2.3
Ca %	0.63	4.90	7.8	2.10	1.20	59	1.3–1.7	174.7	2.5–3.3
Ce	57.00	178.00	3.1	98.00	27.00	28	0.8–0.9	28.8	1.2–1.7
Co	13.60	76.00	5.6	43.50	22.00	50	2.0–2.1	139.2	3.0–4.4
Cr	68.00	200.00	2.9	119.00	36.00	30	1.4–1.4	65.3	2.1–3.1
Cs	0.37	5.50	15.0	2.90	1.60	55	1.0–1.4	6.5	1.8–2.6
Cu*	54.00	1,980.00	37.0	630.00	440.00	70	10.5–12.5	311.8	18.3–24.8
Dy	2.50	13.50	5.4	7.30	2.30	31	0.9–1.2	42.4	1.6–2.3
Eu	1.40	3.50	2.5	2.00	0.41	20	0.8–1.0	39.0	1.3–2.0
Fe %	5.16	12.20	2.4	8.00	2.00	25	1.1–1.3	57.8	1.7–2.5
Hf	4.20	12.80	3.0	6.40	1.70	27	1.0–1.2	42.4	1.5–2.3
K %	0.52	2.89	5.6	1.70	0.53	32	1.0–1.4	29.3	1.4–2.6
La	24.90	84.30	3.4	43.00	13.00	31	0.8–0.9	29.9	1.2–1.8
Lu	390.00	906.00	2.3	560.00	130.00	23	0.8–1.0	33.5	1.3–2.0
Mn	1,300.00	2,750.00	2.1	1,820.00	320.00	17	1.5–1.8	36.6	2.7–3.3
Na %	0.50	1.90	3.7	0.96	0.35	37	1.5–1.5	92.7	2.2–3.3
Nd	18.00	79.00	4.4	44.00	13.00	30	0.6–1.0	30.2	1.1–1.9
Rb	17.40	95.00	5.4	63.00	20.00	31	0.9–1.2	20.5	1.5–2.3
Sc	12.70	37.70	3.0	22.00	7.10	32	1.2–1.3	72.1	1.9–2.8
Sm	6.05	15.70	2.6	8.90	2.00	23	0.8–0.8	30.8	1.2–1.8
Ta	0.67	3.10	4.6	1.10	0.48	42	0.9–1.1	60.8	1.4–2.2
Tb	0.90	2.40	2.6	1.20	0.30	24	0.9–1.0	38.7	1.3–2.0
Th	2.96	20.20	6.8	8.80	2.90	34	0.9–1.0	18.0	1.3–2.0
Yb	2.40	6.20	2.6	3.50	0.80	23	0.9–1.0	37.1	1.3–2.2
Zn	97.00	460.00	4.8	220.00	82.00	37	1.6–2.1	66.6	3.3–4.7

*Determined on acid extracts by atomic adsorption spectrophotometry (AAS).

The average concentrations of 26 elements in both $< 1 \mu\text{m}$ and $< 177 \mu\text{m}$ fractions for the Point Mills stamp sand sample (Franklin #2 conglomerate lode) are given. Notable features are the relatively high concentrations of barium, cerium, chromium, copper, iron, manganese, titanium, vanadium, and zinc. Several rare earth elements of the lanthanide series (cerium, dysprosium, europium, lanthanum, lutetium, neodymium, samarium, tantalum, terbium, ytterbium) are present in addition to hafnium, rubidium, scandium, thorium, and vanadium. Cesium (almost exclusively stable ^{133}Cs) is indicated at modest to low concentrations.

Enrichment values (relative to background) suggest which elements are likely to be enriched (values > 1) by discharges of the conglomerate lode “slime clays” and which are likely to be diluted

(values < 1). Copper stands out among all elements for its highly enriched values in stamp sands relative to background sediments (Point Mills conglomerate, $< 1 \mu\text{m}$, 210X; $< 177 \mu\text{m}$, 62X), followed by a suite of elements that show modest enrichment (2 to 3X; Na, Zn, Co, Ta, Dy, Ha, Yb), and some that are noticeably underrepresented (0.8 to 0.2X; Ru, Mn, As, Cs).

End-member Analysis

The detailed elemental signatures from INAA revealed that the slime clay fraction of different stamp sand piles had distinctive ratios of elements, primarily reflecting the nature of the two major ore lodes (conglomerate and amygdaloid basalt), different from the signature of background sediments (Fig. 10). For example, when elemental concentra-

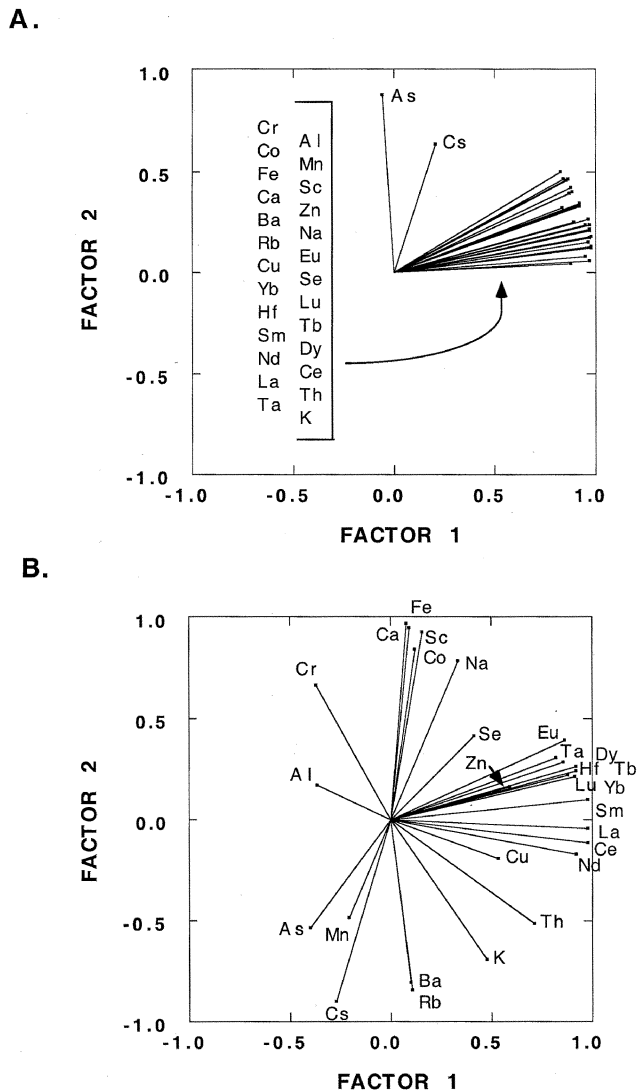


FIG. 9. *Principal Components Analysis for a) elemental flux profiles and b) elemental concentration profile patterns. Elemental profile loadings on factors 1 and 2 are designated by element symbol. The sequence of elements in the large cluster, top figure, is arranged from top to bottom in staggered fashion.*

tions from the Point Mills conglomerate lode (Franklin #2) are divided by elemental concentrations from the Isle Royale amygdaloid lode, certain elements are highly enriched (Th, Nd, La, Ba, Ce), whereas others are moderately enriched (Sm, Tb, Hf, Ta, Yb, Lu, Dy, Eu, Rb). If background concentrations are divided by Point Mills conglomerate values, one element (Cs) is highly enriched.

Three principal sources of sediment to the coring

site were considered: natural pre-mining material (background erosional sediment, represented by premining core strata) and fines from Point Mills (representing the conglomerate lode, a purple color) and Isle Royale (representing the amygdaloid lode, a dark gray color) stamp sands. An end-member analysis (see Methods) was applied to the Portage Lake sediment elemental patterns. The partial mass fluxes for the conglomerate lode, amygdaloid lode, and background (presettlement sediment) elements showed three distinctly different temporal sequences (Fig. 11a).

Background mass flux (erosional input) ranged from 0.03 to 0.04 g/cm²/yr until 1860, then increased exponentially up to maxima of 0.20 to 0.24 g/cm²/yr between 1900 to 1920, followed by a decline and second maximum above 0.20 g/cm²/yr around World War II. Thereafter background mass flux fluctuated between 0.06 to 0.10 g/cm²/yr. Notice that this analysis does not suggest that the erosional signature returned completely back to premining fluxes, rather it remained around 0.07 to 0.10 g/cm²/yr. Historically important contributing factors to accelerated rates would be deforestation associated with mining, dredging associated with Keweenaw Waterway construction and maintenance, and possibly shoreline erosion associated with increased patterns of large ship traffic through the Keweenaw Waterway during strong mining years (1900 to 1920; 1941 to 1945).

The conglomerate lode shows a slower start than the amygdaloid, continual late 1880s increase, followed by maxima of 0.3 to 0.5 g/cm²/yr between 1900 and 1920, a severe dip during maximum production probably indicative of the 1913 strike, then an early decline to baseline conditions in the early 1920s. The conglomerate sequence is very consistent with the historic archived record (Fig. 11b). An early mill, Franklin #1, operated from the 1860s to 1898, whereas the larger Franklin #2 opened in 1898, making an almost continuous transition in stamp sand production. There was a severe dip during maximum production due to the 1913 strike. After 1920, with the closure of the Franklin #2 Mill, processing of conglomerate shifted entirely to the shores of Torch Lake, away from Portage Lake (Kerfoot *et al.* 1994). Although Torch Lake and Portage Lake are connected through the Torch Lake arm of Portage Lake, the restricted conglomerate signature after 1920 suggests that the slime clay fraction discharged from Torch Lake mills did not carry into the central region of Portage Lake. This aspect was also independently verified by showing

TABLE 3. Concentrations of elements and their size-specific enrichment in the clay fraction of Point Mills stamp sand (spit #1, conglomerate lode). Determinations by Instrumental Neutron Activation Analysis, all in $\mu\text{g/g}$ unless otherwise noted (* only approximate ratios).

Element	< 1 μm Mean (SD)	< 177 μm Mean (SD)	Ratio Mean (SD)
Aluminum (%)	6.8 (0.3)	6.1 (0.3)	1.1 (0.1)
Arsenic	3.1 (0.5)	1.9 (0.4)	1.7 (0.4)
Barium	474.1 (43.2)	648.1 (44.8)	0.7 (0.1)
Cerium	130.0 (3.4)	104.0 (2.8)	1.3 (0.0)
Cesium (ppb)	695.1 (137.2)	633.1 (172.8)	1.1 (0.4)
Chromium	86.9 (3.6)	83.5 (3.2)	1.0 (0.1)
Cobalt	35.1 (1.0)	21.0 (0.6)	1.7 (0.1)
Copper (%)	1.7 (0.1)	0.5 (0.0)	3.7 (0.2)
Dysprosium	11.6 (1.2)	9.9 (1.0)	1.2 (0.2)
Europium	2.8 (0.1)	2.6 (0.1)	1.1 (0.1)
Hafnium	10.0 (0.5)	11.5 (0.5)	0.9 (0.1)
Iron (%)	7.6 (0.0)	8.6 (0.0)	0.9 (0.1)
Lanthanum	64.8 (2.1)	48.9 (1.4)	1.3 (0.1)
Lutetium (ppb)	702.2 (71.3)	660.4 (66.3)	1.1 (0.2)
Manganese	1,196.8 (26.3)	826.2 (18.4)	1.4 (0.0)
Molybdenum	< 3.5 (0.2)	< 3.3 (0.2)	*1.1 (0.1)
Neodymium	66.0 (6.8)	47.9 (5.8)	1.4 (0.2)
Potassium (%)	< 1.0 (0.1)	3.2 (0.5)	*.3 (0.1)
Rubidium	66.0 (13.1)	36.7 (10.5)	1.8 (0.6)
Samarium	14.5 (0.7)	12.1 (0.6)	1.2 (0.1)
Scandium	23.1 (0.7)	17.8 (0.6)	1.3 (0.1)
Silver	21.5 (1.0)	7.9 (0.9)	2.7 (0.3)
Sodium (%)	1.8 (0.1)	1.9 (0.1)	0.9 (0.1)
Tantalum	1.7 (0.1)	2.4 (0.1)	0.7 (0.1)
Terbium	1.9 (0.1)	1.6 (0.1)	1.1 (0.1)
Thorium	8.2 (0.2)	7.8 (0.2)	1.0 (0.0)
Titanium	8,593.7 (710.2)	10,932.0 (716.4)	0.8 (0.1)
Uranium	2.8 (0.1)	2.6 (0.1)	1.1 (0.1)
Vanadium	183.3 (6.1)	178.8 (5.9)	1.0 (0.0)
Ytterbium	5.4 (0.3)	5.5 (0.3)	1.0 (0.1)
Zinc	290.0 (16.3)	131.3 (10.2)	2.2 (0.2)

that the characteristic purple slime clays of Torch Lake sediments do not extend very far along the Torch Lake arm into Portage Lake.

The amygdaloid lode partial flux pattern shows an early rise to $0.06 \text{ g/cm}^2/\text{yr}$ in the 1880s followed by a major 1890s fall (Fig. 11a). Mass flux picks up again around 1889, increases with fluctuation to a maximum value of $0.76 \text{ g/cm}^2/\text{yr}$ in the late 1910s, then declines precipitously in the 1920s and 1930s. Flux increases to a secondary maximum of $0.15 \text{ g/cm}^2/\text{yr}$ during the mid-1940s, then relaxes to a value between 0.02 and $0.03 \text{ g/cm}^2/\text{yr}$.

The amygdaloid mass flux also corresponds closely to the documented historic record (Fig. 11b). There were several early small mill amyg-

daloid operations in the 1860 to 80s (Pewabic and Quincy Mills in Hancock; Columbian Mill and Sheldon/Douglas Isle Royale #1 stamp mill at Houghton, additional amygdaloidal input from the Atlantic Mill). These were curtailed by economically driven mill shutdowns and by the 1890 U.S. Army Corps restrictions that limited discharges along the Houghton/Hancock shoreline (Kerfoot *et al.* 1994). The larger Isle Royale #2 mill opened at a different site, closer to Portage Lake, between 1901 and 1947. Stamp discharges from amygdaloid lodes reached a maximum peak between 1910 and 1920s, due to the combined input of the Isle Royale and Centennial operations, declined in the Great Depression, then showed a secondary peak through

TABLE 4. Concentrations of elements and their size-specific enrichment in the clay fraction of Isle Royale stamp sand (amygdaloid lode). Determinations by INAA, all in $\mu\text{g/g}$ unless otherwise noted (* only approximate ratios).

Element	< 1 μm Mean (SD)	< 177 μm Mean (SD)	Ratio Mean (SD)
Aluminum (%)	8.2 (0.3)	8.1 (0.3)	1.0 (0.1)
Arsenic	12.0 (0.9)	9.1 (0.8)	1.3 (0.2)
Barium	74.3 (34.2)	< 122.3 (4.5)	*0.6 (0.3)
Cerium	21.6 (1.2)	29.7 (1.3)	0.7 (0.1)
Cesium (ppb)	737.0 (170.5)	< 604.2 (19.1)	*1.2 (0.3)
Chromium	167.2 (4.7)	151.4 (4.7)	1.1 (0.0)
Cobalt	52.3 (1.5)	41.4 (1.2)	1.3 (0.1)
Copper (%)	0.4 (0.0)	0.1 (0.0)	2.8 (0.7)
Dysprosium	4.3 (0.8)	4.6 (0.9)	0.9 (0.3)
Europium	1.1 (0.1)	1.6 (0.1)	0.7 (0.0)
Hafnium	2.70 (0.3)	2.2 (0.2)	1.2 (0.2)
Iron (%)	7.8 (0.0)	7.5 (0.0)	1.0 (0.0)
Lanthanum	8.8 (0.3)	14.6 (0.4)	0.6 (0.0)
Lutetium (ppb)	256.0 (33.0)	229.3 (26.0)	1.1 (0.2)
Manganese	1,585.6 (34.6)	1,265.9 (27.8)	1.3 (0.0)
Molybdenum	< 2.9 (0.2)	< 3.0 (0.2)	*1.0 (0.1)
Neodymium	6.1 (3.2)	13.3 (3.9)	0.5 (0.3)
Potassium (%)	< 1.0 (0.1)	0.7 (0.3)	*1.5 (0.6)
Rubidium	< 26.6 (1.8)	< 26.1 (1.8)	*1.0 (0.1)
Samarium	3.4 (0.2)	4.6 (0.2)	0.70 (0.1)
Scandium	25.7 (0.8)	28.3 (0.9)	0.9 (0.0)
Silver	3.3 (0.9)	< 3.4 (0.0)	*1.0 (0.3)
Sodium (%)	1.7 (0.1)	1.7 (0.1)	1.0 (0.1)
Tantalum	0.5 (0.1)	0.4 (0.1)	1.2 (0.2)
Terbium	0.5 (0.1)	0.6 (0.1)	0.8 (0.1)
Thorium	0.8 (0.1)	< 0.5 (0.0)	*1.5 (0.2)
Titanium	8,036.9 (691.3)	8,773.4 (671.6)	0.9 (0.1)
Uranium	0.1 (0.1)	< 0.3 (0.0)	*0.5 (0.3)
Vanadium	209.8 (6.8)	214.9 (6.8)	1.0 (0.0)
Ytterbium	1.9 (0.1)	2.2 (0.1)	0.9 (0.1)
Zinc	372.8 (20.3)	111.3 (10.3)	3.4 (0.4)

World War II exclusively from the Isle Royale Mill. The post-1947 inputs of 0.02 to 0.03 $\text{g/cm}^2/\text{yr}$ probably derive from shoreline erosion of existing Isle Royale and Centennial stamp sand piles and yearly application of Isle Royale stamp sands on local highways.

The agreement between lode discharges and slime clay component loadings seems very good. The only major differences are 1) the lower values of slime clays received from the early mill discharges (1860 to 1900), expected because these mill locations were more distant from the center of Portage Lake than later mills, and 2) the clean cut-offs in discharge records, contrasted with the continual post-mill input of amygdaloid slimes by shoreline erosion of stamp sand piles and yearly

highway applications. Otherwise, the end-member analysis provided an excellent reconstruction, emphasizing the historical contrast in discharges between the amygdaloid and conglomerate fractions.

DISCUSSION

Lake sediments are valuable because they archive continuous records of physical, chemical and biotic variables before, during, and after perturbations (Haworth and Lund 1984, DeAngelis 1992). Information from flux and concentration profiles complement each other, increasing understanding of long-term changes in biotic and geological variables (pollen, Davis 1968, Davis and Deevey 1964, zooplankton, Kerfoot 1995; elements linked to basin erosion, Likens and Davis 1975; metals, Rob-

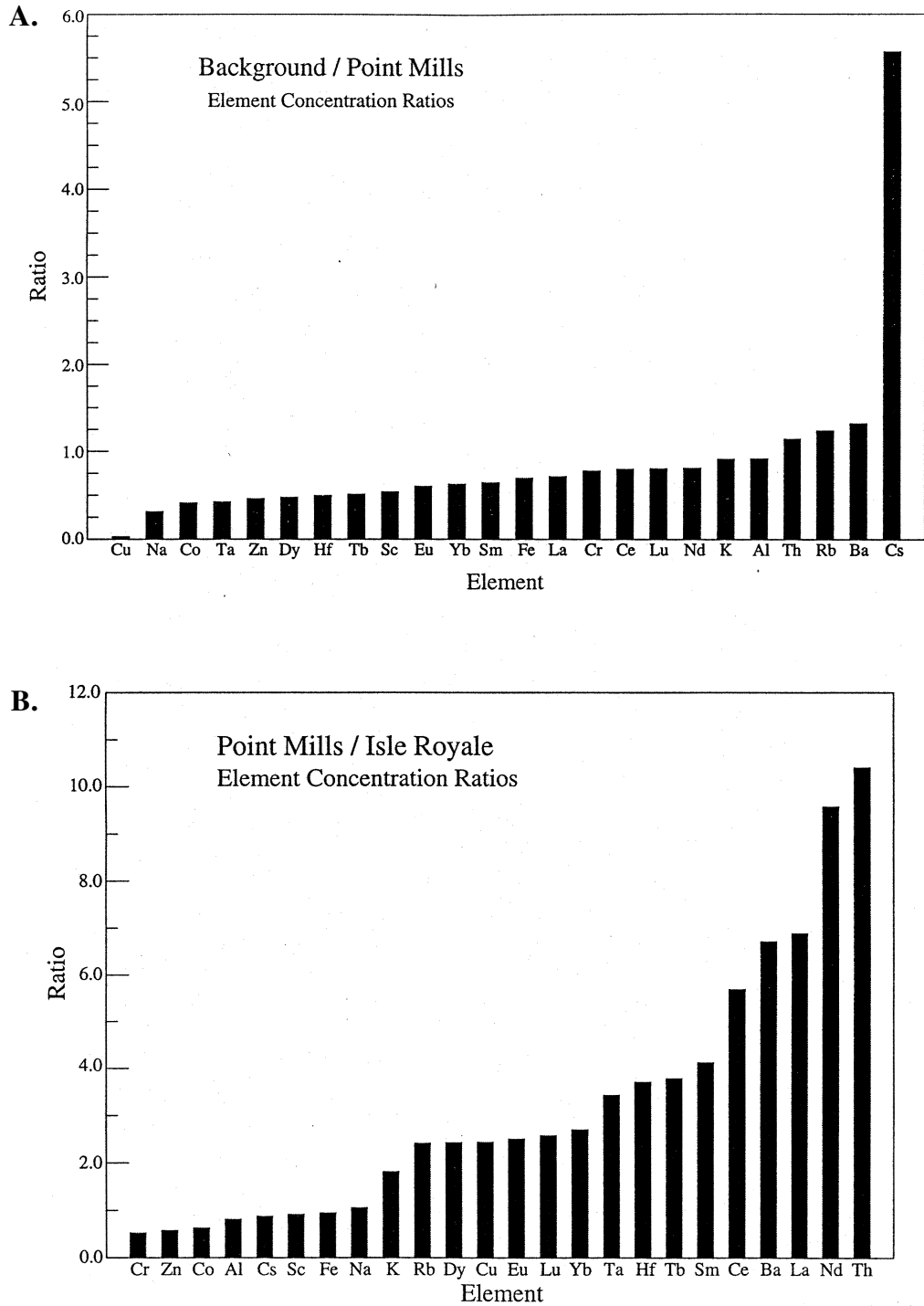


FIG. 10. Differences in the elemental composition of stamp sand and pre-mining sediment samples: a) elemental concentrations of background Portage Lake sediment (BG, pre-mining erosion) divided by Point Mills stamp sand concentrations (PM, conglomerate); same for Point Mills stamp sand divided by Isle Royale stamp sand elemental concentrations (IR, amygdaloid).

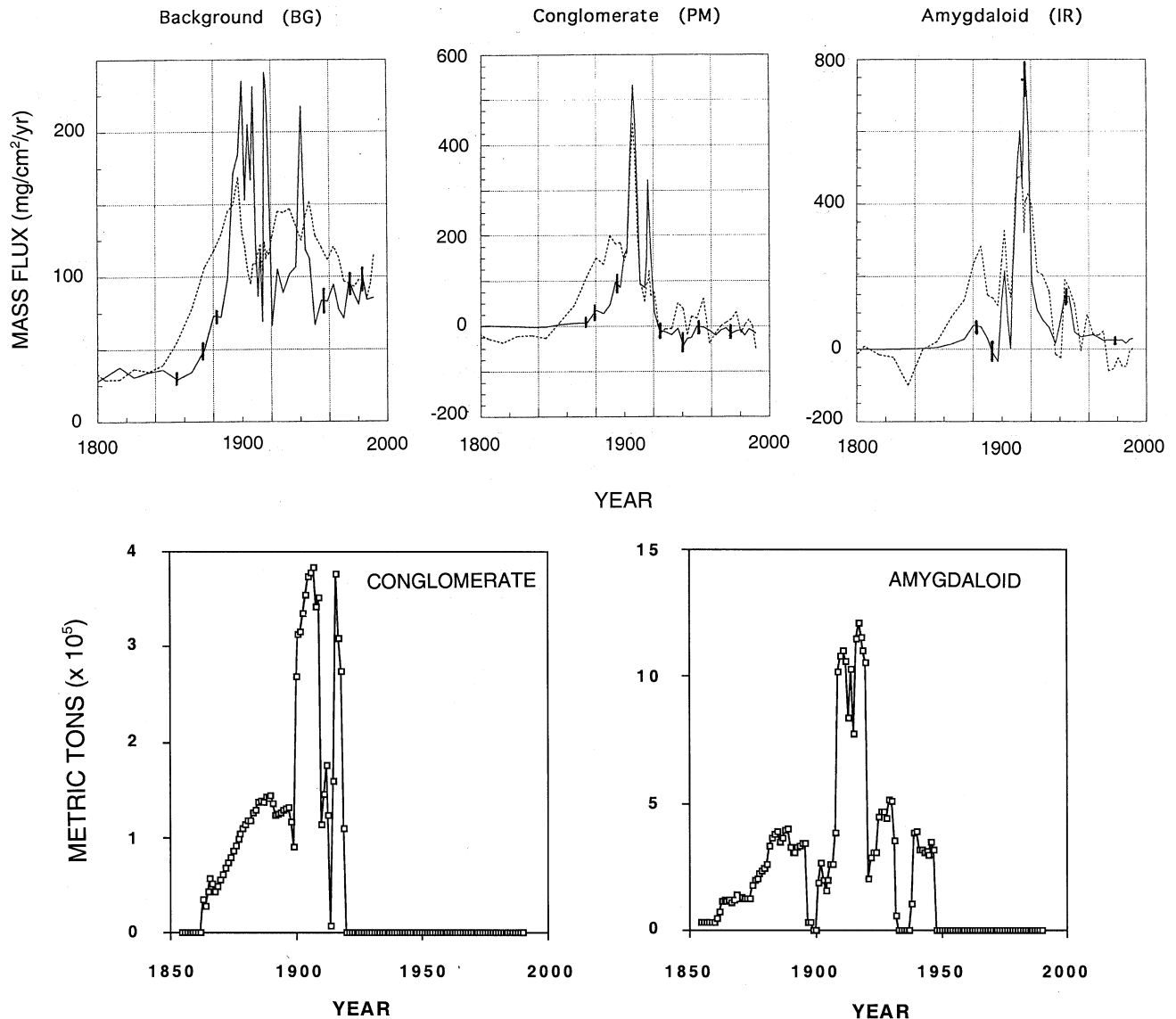


FIG. 11. Comparison of reconstructed source contributions and historical discharge records: a) PCA scores (dashed) and end-member analysis (solid) of Portage Lake core #3 plotted as contributions from three sources: background, conglomerate (Franklin #2; Point Mills), and amygdaloid (Isle Royale); horizontal bars are standard deviations calculated by Monte Carlo methods; b) reconstructed discharge record for conglomerate and amygdaloid lodes from MTU Archive records.

bins *et al.* 1989). In the low-energy Keweenaw Waterway region, the slime clay laminations allow reconstruction of detailed flux and concentration chronologies, approaching the detail from natural varve deposits (O'Sullivan 1983, Saarnisto 1986). However, the process of sediment focusing potentially introduces complications (Lehman 1975, Robbins and Edgington 1975, Davis and Ford 1982, Davis *et al.* 1984, Hilton *et al.* 1986). Fortunately in this case, radioisotopes and direct observations of

laminae thicknesses also allow estimates of this process.

Because the Keweenaw Waterway and Portage Lake were highly perturbed, at first glance it was uncertain that ²¹⁰Pb could be used as a conventional dating tool. Although bioturbation of sediments during mill discharges could be ruled out because of an inhospitable benthic environment and well-preserved varves, other conditions required to develop a valid chronology might not be met. Most

notable is the requirement that the flux of ^{210}Pb to sediments be constant over time under conditions of wildly variable mass loadings. Although it was previously shown that the ^{210}Pb chronology in the vicinity of the top of the core (upper 10 cm) agreed with that based on the location of peak radiocesium (Kerfoot *et al.* 1994), one important finding of the present study is the consistency of the excess ^{210}Pb flux in the presence of major system perturbations.

The inventory (vertically integrated amount) of ^{210}Pb , 80 ± 3 dpm/cm², exceeds the value expected from direct cumulative atmospheric deposition (about 48 dpm/cm², corresponding to a mean atmospheric flux of 1.5 dpm/cm²/yr). However, the inventory ratio for excess ^{210}Pb of $80/48 = 1.7$ is consistent with that obtained for fallout ^{137}Cs . The inventory for ^{137}Cs in core PL3 is 36.8 ± 0.4 dpm/cm² compared to a decay-corrected time integrated rate of radiocesium deposition of 28.5 dpm/cm². The latter yields an inventory ratio of $36.8/28.5 = 1.3$. Since both ^{210}Pb and ^{137}Cs inventory ratios are comparable, the watershed contribution is likely to be small for both nuclides. Elevated inventory ratios probably do not reflect additions from external sources, particularly the watershed, but reflect horizontal redistribution and focusing of the nuclides within the lake. This implies that the inventory ratio is correctly interpreted as a focusing factor of about 1.3 to 1.7.

Laminae thickness over the entire Portage Lake basin allows an independent measure of sediment focusing. Over the 1900 to 1919 interval, regressions of thickness on distance (km) from the central basin are highly significant ($N = 10$, $\text{Depth} = 12.47 - 1.692X$, $R^2 = 0.675$, $P < 0.01$). Ratios of perimeter to central depression thicknesses fall between 2.2 and 1.6, comparable to the above radiometric estimates of radiotracer focusing. Thus radiotracer focusing is consistent with yearly sediment deposition and suggests that ^{210}Pb adsorbed uniformly onto suspended clay particles. In Portage Lake sediments, the cycling of certain elements in the ecosystem was swamped by the physical settling of particles onto bottom sediments. However, today as the mass accumulation rate is returning to near background conditions, fluxes of certain metals (Cu, Zn, Co, Mn, Fe) and associated elements (As) remain elevated considerably above background levels. These very elements were the ones originally enriched in the clay particle fraction of the stamp discharges, underscoring their chemical mobility. It is tempting to suggest that prolonged, ac-

celerated cycling in this suite of elements in the regional environment may be chemically and biologically mediated, through ultraviolet radiation and redox interactions with dissolved organic matter (McKnight and Morel 1979, Moffett and Brand 1996, Scully *et al.* 1996). These intriguing processes, however, go beyond the scope of the present paper, although some specific elements merit further comment.

Principle Component Analysis of concentration profiles helped identify some redox-sensitive (Mn) and dilution-sensitive elements. Proportional enrichment of a few elements after 1920 in the sediment core suggests postdepositional mobility. For example, enrichment patterns suggest movement of Mn. The enrichment of Mn and Fe in near-surface layers of sediment cores is a phenomenon common in Great Lakes sediments and particularly striking in low-deposition, deep-water, Lake Superior cores (McKee *et al.* 1989a,b; Olivarez *et al.* 1989; D. Long, personal communication). Arsenic is also likely to form pH and redox-gradient concentration peaks (D. Long, personal communication) and this property also may account for the peculiar distribution of As in the Portage Lake sediments.

Evidence for direct transport and deposition of the slime clay fraction in Lake Superior is increasing. Recent coring in Keweenaw Bay revealed slime clay laminae also in L'anse Bay, off Baraga, suggesting a straightforward extrapolation of Portage Lake techniques to sheltered bay waters of Lake Superior. Apparently, although summer waters circulate in a relatively higher energy environment than that found in the Keweenaw Waterway, winter discharges by stamp mills under the extensive ice cover of Keweenaw Bay formed buried slime clay laminae at high deposition sites in L'anse Bay and along the Keweenaw Trough. Preliminary work at three locations, one of five cores from L'anse Bay (e.g. LB3-LS95), one at mid-bay (KB LS83) show elevated Cu profiles (Fig. 12, also see Kerfoot *et al.* 1999). Most cores show background copper concentrations generally fluctuating between 20 and 40 $\mu\text{g/g}$. Cu increases early, reaches a buried maximum, then declines in surface strata. Maximum copper concentrations in the buried maximum are highest at the southern Keweenaw Bay site (350 to 700 $\mu\text{g/g}$) and intermediate at mid-bay (230 to 350 $\mu\text{g/g}$) sites. Preliminary ^{137}Cs dating suggests that the buried copper maxima coincide with the 1900 to 1930s discharges at the Gay, Michigan, and Mass Mills along the western shoreline of Keweenaw Bay. Whitefish Bay and Lake George cores (St.

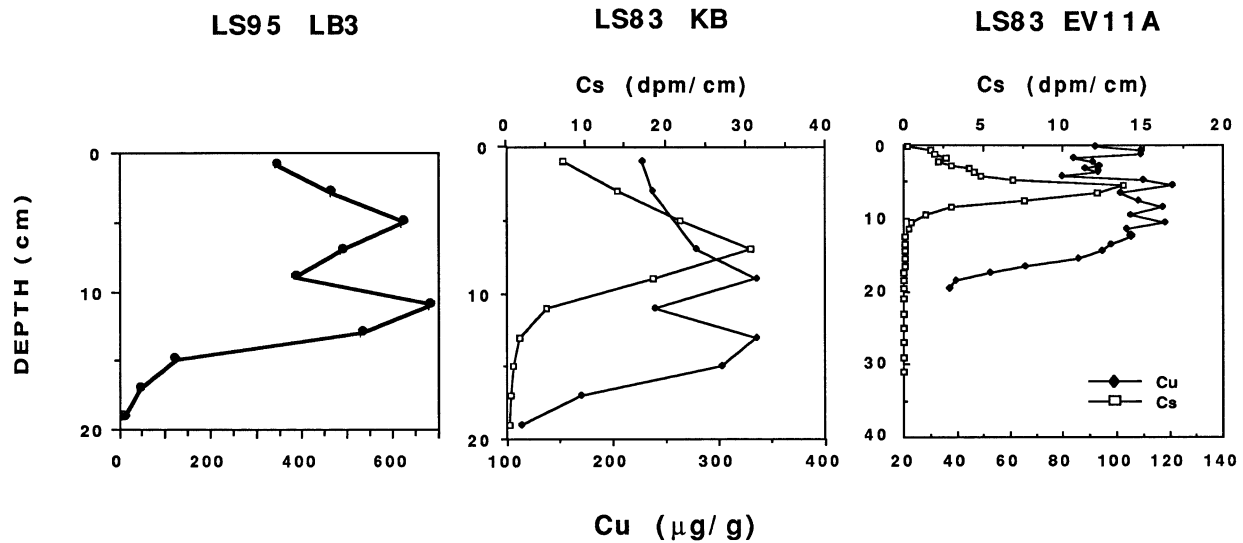


FIG. 12. Comparison of copper concentration profiles in Keweenaw Bay (LB-3, KB) and more eastern sediments (Whitefish Bay, EV11A). Preliminary ^{137}Cs profiles are shown for two of the locations (KB, EV11A). The latter cores collected courtesy of CCIW and CSS LIMNOS.

Marys discharge of Lake Superior; Robbins and Kerfoot unpublished) suggest a 10 to 20 year time lag in the copper pulse, indicative of progressive counterclockwise movement of mining-derived materials by nearshore currents, analogous to the same process uncovered in southern Lake Michigan (Robbins and Edgington 1975, Eadie and Robbins 1987).

Nussman (1965) and Kemp *et al.* (1978), early investigators of Lake Superior sediments, suspected that postsettlement copper enrichments in sediments came from several intensively mined regions: the Keweenaw Peninsula, Thunder Bay, Marathon, and Sault Ste. Marie areas. Many of the metals and other elements enriched in present Keweenaw stamp sand clays and lake sediments (Cu, Zn, As, Mo, Cd) are also characteristically enriched in profile patterns found across eastern basin nearshore sediments. For example, profiles for Zn, Mo, and Cd also are similar to copper (Kemp *et al.* 1978). Recent work on 32 short cores from Lake Superior (Harting *et al.* 1996, Kerfoot *et al.* 1999) clearly indicates that Cu profiles and Cu/Zn ratios are consistent with widespread turn-of-the-century dispersal of slime clay particles along the nearshore coastal currents of the eastern basin and continued broadcasting of the Freda/Redridge Mill discharges into more interior regions by the Keweenaw Current. The interactions between the historical nearshore

movement of clay-sized “slime” particles and the more dissolution-dominated environments in offshore waters and at offshore sediment-water interfaces raises several intriguing questions for future research.

SUMMARY AND CONCLUSIONS

The Keweenaw Waterway record is important for two reasons: 1) the sedimentary record traces the regional ecosystem impacts of turn-of-the-century native copper mining almost full cycle, i.e., through reforestation and the return of mass sedimentation rates to near-background conditions, and 2) the strata have remained in place. The historical flux profiles document the accelerated elemental inputs into Portage Lake and collectively provide a signature for the native copper mining perturbation. INAA techniques “fingerprinted” source materials distinguishing “slime” clay contributions from two primary ore loads (conglomerate, amygdaloid), each transported up to 3 km from more remote discharge sites. Moreover, the historic link between mining operations, historic perturbations to the lake, and material transport could be directly verified through archived production records.

Whereas factor analysis is routinely applied to sort out variables, here the application literally tied fluxes to physical loading factors. Factor analysis suggested ties with ore loads and background sedi-

mentation. If anything, the factor loadings did as good a job of reconstructing early recorded discharge patterns as the end-member analysis. Linear regressions between the end member mass fluxes (three characterized source materials) and each factor score profile showed relatively high correlations (Point Mills conglomerate 0.84; Isle Royale amygdaloid 0.81; background sediment composition 0.63). The elemental composition of ore sources was sufficiently distinct that a more direct end-member analysis successfully distinguished inputs from various ore sources. The multi-element partial fluxes were verified through archived mill production records.

Thus it was shown that multivariate techniques hold promise for tracing "signatures" of mining-discharged particles in high sedimentation regions of Lake Superior sediments. In the low-energy environment of Portage Lake, Principal Components Analysis also helped to highlight "non-conforming" elements.

ACKNOWLEDGMENTS

This research was supported by NSF OCE97-12827 to WCK and by two Michigan Great Lakes Protection Fund awards, #910417 and #090192, to WCK and JR, administered by the Michigan Department of Natural Resources, Lansing, Michigan. Special thanks go to Susan Savage for graphs of element profiles. We are grateful for the help of Nancy Moorehead (GLERL) in making radiometric measurements and R. Rood (GLERL) and E. Bird-sall at the Phoenix Memorial Laboratory, University of Michigan, for generating neutron activation data. Lynn Herche assisted in the factor analysis and Kerry Kosnak helped with the MTU Archives search and amygdaloid/conglomerate loadings. Sandra Harting provided personal data for use in Figure 12. Lake Superior sediment cores collected during CSS LIMNOS cruise (National Water Research Institute, Burlington, Ontario, 12–22 July 1983). Gerald Ankley (USEPA-Duluth), Sandra Harting, Susan Savage, and Lucille Zelazny made comments on manuscript drafts. We also gratefully acknowledge the helpful and detailed comments of outside anonymous reviewers. Contribution No. 1152, Great Lakes Environmental Research lab.

REFERENCES

- Babcock, L.L., and Spiroff, K. 1970. *Recovery of copper from Michigan stamp sands. Volume I. Mine and mill origin, Sampling and mineralogy of stamp sand.* Institute of Mineral Research, Michigan Technological University, Houghton, MI.
- Benedict, C.H. 1952. *Red Metal—The Calumet and Hecla Story.* Ann Arbor, Michigan: University of Michigan Press.
- . 1955. *Lake Superior Milling Practice.* Houghton, Michigan: Michigan College of Mining And Technology Press.
- Dams, R.A., and Robbins, J.A. 1970. *Non-destructive activation analysis of environmental samples.* Spec. Rep. 48, Great Lakes Research Division, University of Michigan, Ann Arbor, MI.
- Davis, M.B. 1968. Climatic changes in southern Connecticut recorded by pollen deposition at Rogers Lake. *Ecology* 50:409–422.
- , and Deevey, E.S., Jr. 1964. Pollen accumulation rate: estimates from late-glacial sediment of Rogers Lake. *Science* 145:1293–1295.
- , and Ford, M.S. (J.) 1982. Sediment focusing in Mirror Lake, New Hampshire. *Limnol. Oceanogr.* 27:137–150.
- , Moeller, R.E., and Ford, M.S.(J.) 1984. Sediment focusing and pollen influx. In *Lake Sediments and Environmental History.* eds. E.Y. Haworth and J.W.G. Lund, pp. 261–293. Leicester, England: Univ. Leicester Press.
- DeAngelis, D.L. 1992. *Dynamics Of Nutrient Cycling And Food Webs.* New York: Chapman & Hall.
- Eadie, B.J., and Robbins, J.A. 1987. The role of particulate matter in the movement of contaminants in the Great Lakes. In *Sources and fates of Aquatic Pollutants,* eds. R.A. Hites and S.J. Eisenreich, pp. 319–364. Advances in Chemistry Series No. 216.
- Harting, S., Kerfoot, W.C., Robbins, J.A., and Rossman, R. 1996. Mercury around Lake Superior: Calibrating the historic record. ASLO Abstracts, University of Wisconsin-Milwaukee.
- Haworth, E.Y., and Lund, J.W. (eds). 1984. *Lake sediments and environmental history.* Leicester, England: Univ. Leicester Press.
- Hilton, J., Lishman, J.P., and Allen, P.V. 1986. The dominant processes of sediment distribution and focusing in a small, monomictic lake. *Limnol. Oceanogr.* 31:125–133.
- Kemp, A.L., Williams, J.D.H., Thomas, R.L., and Gregory, M.L. 1978. Impact of man's activities on the chemical composition of the sediments of lakes Superior and Huron. *Water, Air, and Soil Pollution* 10:381–402.
- Kennedy, A.D. 1970. *Recovery of copper from Michigan stamp sands. Vol. II, Physical and chemical properties of stamp sand.* Michigan Technological University, Institute of Mineral Research, Houghton, MI.
- Kerfoot, W.C. 1995. Historical ecology: Coupling remain production to flux calculations in sediment core studies. ASLO Abstracts, University of Nevada, Reno.
- , Lauster, G., and Robbins, J.A. 1994. Paleolimno-

- logical study of copper mining around Lake Superior: Artificial varves from Portage Lake provide a high resolution record. *Limnol. Oceanogr.* 39(3): 649–669.
- , Harting, S., Rossmann, R., and Robbins, J.A. 1999. Anthropogenic copper inventories and mercury profiles from lake Superior: evidence for mining impacts. *J. Great Lakes Res.* 25(4):663–682.
- Lankton, L. 1991. *Cradle To Grave*. Oxford, England: Oxford University Press.
- , and Hyde, C.C. 1982. *Old Reliable: An Illustrated History Of The Quincy Mining Company*. Quincy Mine Hoist Association, Hancock, MI.
- Lehman, J.T. 1975. Reconstructing the rate of accumulation of lake sediment: The effect of sediment focusing. *Quaternary Res.* 5:541–50.
- Likens, G.E., and Davis, M.B. 1975. Post-glacial history of Mirror Lake and its watershed in New Hampshire, U.S.A.: an initial report. *Verh. Internat. Verein. Limnol.* 19:982–993.
- McKee, J.D., Wilson, T.P., Long, D.T., and Owen, R.M. 1989a. Pore water profiles and early diagenesis of Mn, Cu, and Pb in sediments from large lakes. *J. Great Lakes Res.* 15(1):68–83.
- , Wilson, T.P., Long, D.T., and Owen, R.M. 1989b. Geochemical partitioning of Pb, Zn, Cu, Fe, and Mn across the sediment-water interface in large lakes. *J. Great Lakes Res.* 15(1):46–58.
- McKnight, D.M., and Morel, F.M.M. 1979. Release of weak and strong copper-complexing agents by algae. *Limnol. Oceanogr.* 24:823–837.
- Moffett, J.W., and Brand, L.E. 1996. Production of strong, extracellular Cu chelators by marine cyanobacteria in response to Cu stress. *Limnol. Oceanogr.* 41:388–395.
- Mudroch, A., Sarazin, L., and Lomas, T. 1988. Summary of surface and background concentrations of selected elements in the Great Lakes sediments. *J. Great Lakes Res.* 14(2):241–251.
- Nussmann, D.G. 1965. Trace elements in the sediments of Lake Superior. Ph.D. thesis, University of Michigan, Ann Arbor, MI
- Olivarez, A.M., Owen, R.M., and Long, D.T. 1989. Geochemistry of rare earth elements in benthic layer particulate matter and sediments of Lake Superior. *J. Great Lakes Res.* 15:59–67.
- O'Sullivan, P.E. 1983. Annually laminated lake sediments and the study of Quaternary environmental changes- a review. *Quat. Sci. Rev.* 1:245–313.
- Robbins, J.A., and Edgington, D.N. 1975. Determination of recent sedimentation rates in Lake Michigan using ^{210}Pb and ^{137}Cs . *Geochim. Cosmochim. Acta* 39:285–304.
- , and Herche, L.R. 1993. Models and uncertainty in ^{210}Pb dating of sediments. *Verh. Internat. Verein. Limnol.* 25:217–222.
- , Keilty, T.J., White, D.S., and Edgington, D.N. 1989. Relationships between tubificid abundances, sediment composition, and accumulation rates in Lake Erie. *Can. J. Fish. Aquat. Sci.* 46:223–231.
- Saarnisto, M. 1986. Annually laminated sediments. In *Handbook of Holocene Palaeoecology and Palaeohydrology*, ed. B.E. Berglund, pp. 343–370. New York: John Wiley & Sons.
- Scully, N.M., McQueen, D.J., Lean, D.R.S., and Cooper, W.J. 1996. Hydrogen peroxide formation: The interaction of ultraviolet radiation and dissolved organic carbon in lake waters along a 43–75°N gradient. *Limnol. Oceanogr.* 41:540–548.
- Sokal, R.R., and Rohlf, F.J. 1982. *Biometry*. 2nd edition. San Francisco, CA: Freeman and Co.
- Wilband, J.T. 1978. *The Copper Resources of Northern Michigan*. U.S. Dept. Interior.
- Wilkinson, L. 1989. *SYSTAT: The System for Statistics*. Evanston, IL; SYSTAT, Inc.

Submitted: 30 November 1997

Accepted: 5 July 1999